

Updated Response to Reviewer #1's Comments:

Jiayi Li et al. (Author)

We would like to express our sincere gratitude to Reviewer #1 for the insightful and professional comments. We provide the following response to Reviewer #1's comments regarding the data and methods. Additionally, we have incorporated Reviewer #2's suggestions and further refined the results. To ensure consistent responses, we decide to reply to reviewer #1's comments again.

In the following text, the reviewers' comments are listed in black, our response is in blue, and changes to the text are highlighted in red. A version of the revised manuscript with tracked changes is also provided.

Important revision includes:

1. According to Reviewer #1's comments, only the threshold of GPM = 0 mm/hr was used for the exclusion of precipitation. The corresponding result section has been modified. The N_d -LWP relationship no longer exhibits the initial increasing trend in both regions. The quantification of the impact of diurnal variations on radiative effects has been revised.
2. We have clarified the explanation of the mechanisms based on direct conclusions. This allows us to distinguish between these directly supported conclusions and inferences that rely on previous research with supporting evidence.

Specific Responses:

1. The retrievals of cloud properties:

The native resolution of the AHI is 2 km. Why use a microphysical product of 4 km? The low resolution renders the retrieval very sensitive to errors due to partial pixel filling in most cases, except for the fully cloudy scenes. Therefore, the effects of cloud cover are confounded with those on LWP.

Response: Thanks for your great comment. Although the native resolution of AHI is higher, the official AHI dataset only provides the effective radius (r_e) Level-2 product for the 2.3 μm channel. In contrast, the SatCOPRS CERES Geostationary Satellite Edition 4 Himawari-8 product we used (CER_GEO_ED4_HIM08_NH_V01.2, CER_GEO_ED4_HIM08_SH_V01.2) has a coarser resolution but provides r_e Level-2 product for the 3.9 μm channel using the Langley Research Center (LARC)s

SatCORPS algorithms in support of CERES project. This product with the 3.9 μm channel is considered more accurate for cloud droplet number concentration (N_d) retrievals because this channel better represents the cloud-top information, introducing less bias to the retrieval of N_d (25%~38% for 2.3 μm , less than 20% for 3.7 μm according to Grosvenor et al., 2018).

Additionally, the 3.9 μm r_e from CER_GEO_ED4_HIM08 shows good consistency with the 3.7 μm r_e from MODIS (Figure R1), supporting us in obtaining more accurate N_d . While the coarser resolution may impact the retrieval to some extent as the reviewer said, SatCOPRS CERES Geostationary Satellite cloud product only uses cloudy pixels based on the CERES Ed4 cloud mask (Trepte et al., 2019; Yost et al., 2021), thus largely avoiding the situation mentioned by the reviewer.

Considering the overall quality of the product and the existing precedent of using SatCOPRS CERES Geostationary Satellite products in studies for LWP adjustments (Qiu et al., 2024), we finally selected this dataset in our study.

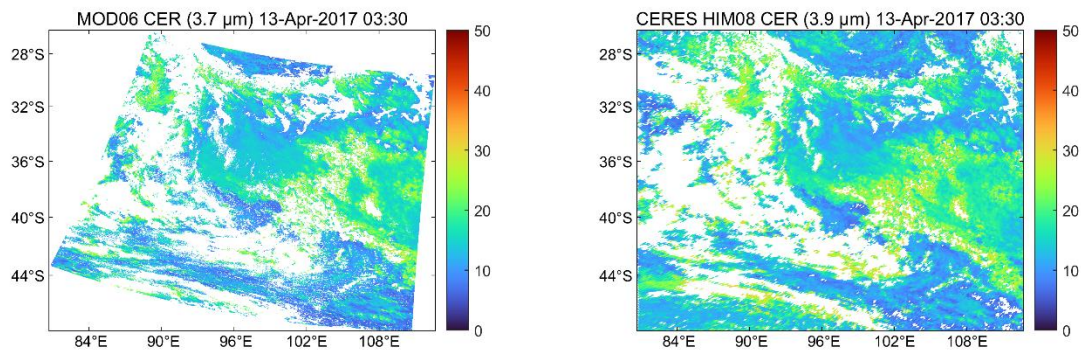


Figure R1. Comparison of the 3.7 μm r_e from MODIS and the 3.9 μm r_e from CER_GEO_ED4_HIM08_SH_V01.2.

Why sub-sampling the data? Why is it 8 km at the NH and 6 km at the SH?

Response: Thank you for raising this question. The description of the data resolution in the manuscript was based on the data introduction available on the NASA EARTHDATA SEARCH ([https://search.earthdata.nasa.gov/search/granules/collection-details?p=C1584977037-](https://search.earthdata.nasa.gov/search/granules/collection-details?p=C1584977037-LARC_ASDC&pg[0][v]=f&pg[0][gsk]=-start_date&fpj=CERES&lat=0.0703125&long=-0.0703125)

[LARC_ASDC&pg\[0\]\[v\]=f&pg\[0\]\[gsk\]=-start_date&fpj=CERES&lat=0.0703125&long=-0.0703125](https://search.earthdata.nasa.gov/search/granules/collection-details?p=C1584977037-LARC_ASDC&pg[0][v]=f&pg[0][gsk]=-start_date&fpj=CERES&lat=0.0703125&long=-0.0703125)).

However, after reaching out to technical staff through the Earthdata forum for clarification, we learned that the information on the website is incorrect. The observation resolution of CERES_GOES_HIM08 is 2 km at nadir, and has been sub-sampled to 6 km for both the Northern and Southern Hemispheres. The sub-sampled resolution meets the needs of the CERES project without having a data implosion.

We provide the link to our post and the related response from the technical staff for the reviewer's

reference (<https://forum.earthdata.nasa.gov/viewtopic.php?t=6315>). We have corrected this issue in the revised version of the manuscript.

2. There is no justification for the threshold of $r_e < 14 \mu\text{m}$. While larger r_e allows more water loss by precipitation, it may be more than balanced by less water loss due to less evaporation of the larger cloud drops.
3. Furthermore, r_e increases with cloud geometrical depth (CGT) and LWP increases with CGT^2 . Therefore, excluding scenes by their r_e values is incurring bias, rendering the whole study questionable
4. Line 131: The positive trend of LWP with N_d was previously documented to occur only at $N_d < 30 \text{ cm}^{-3}$ (Figure 2 of Gyspeerd et al., 2019). The clouds have to be very shallow with respectively small LWP for $r_e < 14$ in clouds with $N_d < 30 \text{ cm}^{-3}$.

In fact, the condition of $r_e < 14 \mu\text{m}$ imposes an artifact of more LWP with larger N_d , because with larger N_d the cloud needs to grow deeper and have larger LWP for reaching $r_e = 14 \mu\text{m}$ at the cloud top !!!

1. Indeed, this study's maximum LWP is shifted from 30 (Figure 2 of Gyspeerd et al., 2019) to nearly 100 cm^{-3} . This is evident in Fig1 left panels, especially in the convective regime (AUW), where cloud thickness and, hence, LWP consistently increase with N_d . This artifact dominates the results of this study.

Response: We agree with this great point, and we sincerely appreciate the reviewer's professional comments. Since these comments all relate to the threshold of $r_e < 14 \mu\text{m}$, we will address this point below.

This issue was discussed earlier in the study. The reason for choosing the threshold of $r_e < 14 \mu\text{m}$ is that the invalidation of adiabatic assumptions for N_d retrievals under precipitation conditions can introduce bias. For example, Grosvenor et al. (2018) suggests in their review paper on N_d retrieval that "As a precautionary measure, it may be prudent to attempt to filter out situations with precipitation before performing N_d retrievals". Kang et al. (2021), using aircraft observations, also pointed out that removing precipitation enhances the retrieval accuracy of r_e in SatCORPS Himawari-8 product, which is an important variable affecting N_d retrieval. Therefore, in order to obtain more accurate N_d values and focus on the microphysical processes within non-precipitating clouds, we firstly used GPM IMERG hourly precipitation product to exclude precipitation scenes. However, considering GPM's limited ability to detect light drizzle, we additionally applied $r_e < 14 \mu\text{m}$ threshold based on suggestions according to

Rosenfeld et al. (2012), which has been widely used to distinguish between precipitating and non-precipitating clouds (Possner et al., 2020; Rosenfeld et al., 2019).

We acknowledge the reviewer's concern on using the threshold of $r_e < 14 \mu\text{m}$. The sensitivity analysis on whether to exclude precipitation has been conducted. Figure R2 shows the N_d -LWP relationship and the diurnal variations LWP adjustments under different precipitation criteria. In both regions, the threshold application primarily removes cloud samples with small N_d and large LWP, located in the upper left of the N_d -LWP space. Specifically, in AUW region, the diurnal pattern shows little change before noon, and without the threshold of $r_e < 14 \mu\text{m}$, the afternoon variation becomes smaller, indicating that the samples we excluded primarily affected the afternoon results. This may be because clouds with larger r_e and larger LWP primarily occur in the afternoon. In the morning, r_e is relatively small, so adding the threshold of $r_e < 14 \mu\text{m}$ does not significantly affect the dominant samples. However, in the afternoon, as r_e increases, the inclusion of samples with smaller N_d and larger LWP causes the LWP adjustments to become more negative. The results using only GPM criterion are similar to those without any precipitation restriction, indicating the diurnal pattern is dominated by non-precipitating samples. In the ECS region, adding the threshold of $r_e < 14 \mu\text{m}$ has little impact on the diurnal pattern of LWP adjustments, mainly affecting the values. This is likely because the ECS region is characterized by smaller r_e values with heavily influence by anthropogenic aerosol pollution. Most precipitation samples are excluded by GPM.

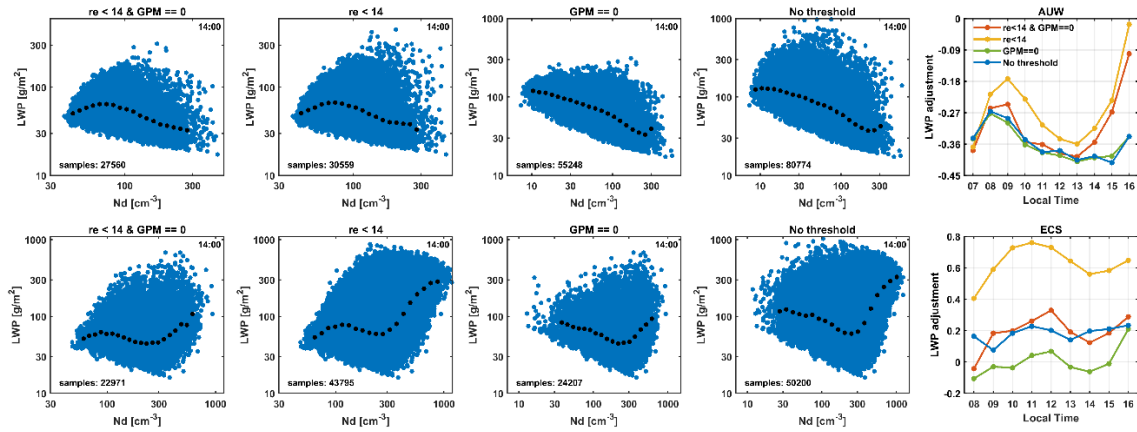


Figure R2. Comparison of the N_d -LWP relationship and diurnal variations of LWP adjustments under different precipitation screening criteria in two typical regions (the west of Australia, AUW and the east China sea, ECS). Blue dots are all sample within the N_d -LWP space at 1400 LT. Black dots represent median LWP in each N_d bin.

Based on the results of the above sensitivity analysis, and considering the aim to minimize the significant uncertainties that heavy precipitation may introduce to the retrieval of N_d . We have decided not to use the $r_e < 14 \mu\text{m}$ threshold following the reviewer's suggestion, but we still retain the exclusion of heavy precipitation scenes with the criteria of $\text{GPM} = 0$.

Combining feedbacks from both reviewers, the updated results are provided in the revised manuscript. Overall, the primary conclusions have been revised to (see Lines 510-538): "This study reveals the diurnal variations of LWP adjustments in two specific regions within the sight of Himawari-8, along with the possible mechanisms contributing to these variations. The studied regions have significant differences in environmental conditions and aerosol loadings. Although some conclusions are similar to the previous studies, we have also discovered some new phenomena. The observational studies demonstrate LWP adjustments in two regions are determined by the dominant microphysical-dynamical processes in different N_d stages (entrainment feedbacks and warm invigoration), while their diurnal variations depend on the dynamical conditions of the boundary layer. Important findings from this investigation are as follows:

- (1) In AUV region, the diurnal variations of LWP adjustments are insensitive to seasonality. The overall negative LWP adjustments decrease from -0.27 to -0.41 before 1300 LT and then increase to -0.34 . Cloud thickness in AUV region can serve as a confounder to separate the effects of meteorological covariations. The diurnal pattern is primarily associated with cloud thinning induced by decoupling process of MBL quantified by LWP skewness before 1300 LT and the weakening of entrainment induced by intensification of large-scale subsidence after 1300 LT.
- (2) In ECS region, diurnal variations of LWP adjustment exhibit seasonal differences. Samples from winter and spring dominate the overall variations (accounting for 75% of the total samples). For the overall results, LWP increases and then decreases with N_d , suggesting possible competition between entrainment feedbacks and warm invigoration. The diurnal pattern of LWP adjustments is determined by the combined diurnal variations of these two mechanisms. Warm invigoration is related to the diurnal variation of the N_d at the turning points of the two processes. Lower N_d in the ECS region implies a weaker warm invigoration.
- (3) We indicate an overall underestimation of the cooling effect by LWP adjustment up to 89% (14%), with a further 20% (15%) offset of the Twomey effect when neglecting the diurnal

variations of LWP adjustments in AUW (ECS) region. Furthermore, our results quantify the regional impact of boundary layer dynamic conditions on LWP adjustments. For example, diurnal decoupling process in AUW region results in a 219% variation of LWP adjustments within the daytime relative to the daily mean (the diurnal variation range divided by the daily mean), assuming other conditions remain relatively unchanged.

Our research provides a detailed discussion for the diurnal variations of LWP adjustments and how they are influenced by existed boundary layer mechanisms. We underscore the importance of fully considering the covariation with environmental conditions, indicating different potential influencing factors on cloud brightening and radiative forcing in terms of the regional and diurnal daytime scale. It is a highly time-dependent variable lacking quantification and should be taken into consideration of future research in aerosol indirect effects on climate.”.

Reference

- Bennartz, R.: Global assessment of marine boundary layer cloud droplet number concentration from satellite, *J. Geophys. Res.*, 112, D02201, <https://doi.org/10.1029/2006JD007547>, 2007.
- Grosvenor, D. P., Sourdeval, O., Zuidema, P., Ackerman, A., Alexandrov, M. D., Bennartz, R., Boers, R., Cairns, B., Chiu, J. C., Christensen, M., Deneke, H., Diamond, M., Feingold, G., Fridlind, A., H  nerbein, A., Knist, C., Kollias, P., Marshak, A., McCoy, D., Merk, D., Painemal, D., Rausch, J., Rosenfeld, D., Russchenberg, H., Seifert, P., Sinclair, K., Stier, P., van Didenhoven, B., Wendisch, M., Werner, F., Wood, R., Zhang, Z., and Quaas, J.: Remote Sensing of Droplet Number Concentration in Warm Clouds: A Review of the Current State of Knowledge and Perspectives, *Reviews of Geophysics*, 56, 409–453, <https://doi.org/10.1029/2017RG000593>, 2018.
- Kang, L., Marchand, R., and Smith, W.: Evaluation of MODIS and Himawari-8 Low Clouds Retrievals Over the Southern Ocean With In Situ Measurements From the SOCRATES Campaign, *Earth and Space Science*, 8, <https://doi.org/10.1029/2020EA001397>, 2021.
- Possner, A., Eastman, R., Bender, F., and Glassmeier, F.: Deconvolution of boundary layer depth and aerosol constraints on cloud water path in subtropical stratocumulus decks, *Atmos. Chem. Phys.*, 20, 3609–3621, <https://doi.org/10.5194/acp-20-3609-2020>, 2020.
- Qiu, S., Zheng, X., Painemal, D., Terai, C. R., and Zhou, X.: Daytime variation in the aerosol indirect effect for warm marine boundary layer clouds in the eastern North Atlantic, *Atmospheric Chemistry and Physics*, 24, 2913–2935, <https://doi.org/10.5194/acp-24-2913-2024>, 2024.
- Rosenfeld, D., Wang, H., and Rasch, P. J.: The roles of cloud drop effective radius and LWP in determining rain properties in marine stratocumulus, *Geophysical Research Letters*, 39, <https://doi.org/10.1029/2012GL052028>, 2012.
- Rosenfeld, D., Zhu, Y., Wang, M., Zheng, Y., Goren, T., and Yu, S.: Aerosol-driven droplet concentrations dominate coverage and water of oceanic low-level clouds, *Science*, 363, eaav0566, <https://doi.org/10.1126/science.aav0566>, 2019.
- Trepte, Q. Z., Minnis, P., Sun-Mack, S., Yost, C. R., Chen, Y., Jin, Z., Hong, G., Chang, F.-L., Smith, W.

L., Bedka, K. M., and Chee, T. L.: Global Cloud Detection for CERES Edition 4 Using Terra and Aqua MODIS Data, *IEEE Transactions on Geoscience and Remote Sensing*, 57, 9410–9449, <https://doi.org/10.1109/TGRS.2019.2926620>, 2019.

Yost, C. R., Minnis, P., Sun-Mack, S., Chen, Y., and Smith, W. L.: CERES MODIS Cloud Product Retrievals for Edition 4—Part II: Comparisons to CloudSat and CALIPSO, *IEEE Transactions on Geoscience and Remote Sensing*, 59, 3695–3724, <https://doi.org/10.1109/TGRS.2020.3015155>, 2021.

Response to Reviewer #2's Comments:

Jiayi Li et al. (Author)

We sincerely appreciate Reviewer #2's insightful suggestions, which prompt us to clarify several points and strengthen the arguments. Overall, we have clarified the explanation of the mechanisms with more supporting evidences. Many detailed discussions as suggested for the conclusion have been provided in the revised manuscript. Furthermore, we have improved the language for greater accuracy and readability.

In the following text, the reviewers' comments are listed in black, our response is in blue, and changes to the text are highlighted in red. A version of the revised manuscript with tracked changes is also provided.

Important revision includes:

1. According to Reviewer #1's comments, only the threshold of $GPM = 0$ mm/hr was used for the exclusion of precipitation. The corresponding result section has been modified. The N_d -LWP relationship no longer exhibits the initial increasing trend in both regions. The quantification of the impact of diurnal variations on radiative effects has been revised.
2. We have clarified the explanation of the mechanisms based on direct conclusions. This allows us to distinguish between these directly supported conclusions and inferences that rely on previous research with supporting evidence.

Major comments:

1. The authors analyze data spanning three entire years, rather than focusing on specific seasons. However, this approach carries some risk because it is well-established that cloud properties and environmental conditions can vary significantly across different seasons. I recommend that the authors examine potential seasonal differences and assess how these variations might influence their results.

Response: We sincerely appreciate the reviewer for highlighting this important consideration regarding the potential seasonal differences. We have conducted further analyses on seasonal sensitivities as suggested (Figures R2-5 compared to Figure R1). Overall, in AUW region the diurnal pattern of LWP adjustments is not sensitive to seasonal changes, while the ECS region exhibits seasonal differences.

Among the total samples (173181), spring, summer, autumn, and winter account for 31%, 3%, 22%, and 44%, respectively. Due to the limited summer samples (3%), their results are statistically insignificant ($p > 0.05$), especially after eliminating the samples with precipitation by applying the threshold ($GPM = 0 \text{ mm hr}^{-1}$). The LWP adjustments in other seasons exhibit similar diurnal patterns and magnitudes, peaking at noon (black lines in Figures R2F, R4-5F). This similarity may be due to the weak seasonal variations in the diurnal patterns of LWP and N_d (Figure R6). The diurnal patterns of warm invigoration in spring and winter are similar to the overall results (blue lines in Figures R2F and R5F compared to Figure R1F). The minimum N_d at 1100 LT coincides with the weakest warm invigoration (i.e., minimal LWP enhancement). Autumn exhibits the lowest N_d among seasons (Figure R4F), corresponding to the weakest warm invigoration (~50%/~31% lower than spring/winter) and the largest diurnal fluctuations. The diurnal pattern of entrainment feedbacks in spring differs from other seasons, possibly due to its distinct entrainment rate diurnal variation, which can be illustrated by the variation of cloud-top height (CLTH). Here, based on the relationship between CLTH, w_s (always negative) and entrainment rate (w_e) ($\frac{dCLTH}{dt} = w_s + w_e$) (Painemal et al., 2013), the diurnal variations of w_e (entrainment rate) can be qualitatively analyzed with the diurnal variations of CLTH and large-scale subsidence (w_s) (Figure R7). Before 1400 LT, the variation of large-scale subsidence is unrelated to CLTH, thus the change in CLTH can only be attributed to entrainment rate. It weakens before 1200 LT, possibly due to the decreasing cloud-top longwave cooling after sunrise. It then increases until 1400 LT which may be caused by the enhanced longwave cooling. After 1400 LT, the decrease in CLTH is caused by the enhancement of large-scale subsidence.

We have added a relevant content of seasonal sensitivity in the revised manuscript (see Lines 420-442):

“Given that the samples include four seasons over four years, we conduct a sensitivity analysis regarding seasonal influences as cloud properties and environmental conditions can vary significantly across different seasons. Overall, the diurnal pattern of LWP adjustments is not sensitive to seasonal changes in AUW region (black lines in Figures S9F-S12F compared to Figure 1). Since the AUW region is a persistent stratocumulus area, the diurnal variations of cloud thickness remain consistent across all seasons, with the thickest clouds in the morning and the thinnest in the early afternoon, followed by a slow increase. This implies that the decoupling process in the persistent Sc region is not affected by seasonality, resulting in the similar patterns of LWP adjustments. ECS region exhibits seasonal

differences (Figures S9-S12). Among the total samples (173181), spring, summer, autumn, and winter account for 31%, 3%, 22%, and 44%, respectively. Due to the limited summer samples (3%), their results are statistical insignificance ($p > 0.05$), especially after eliminating the samples with precipitation by applying the threshold ($GPM = 0 \text{ mm hr}^{-1}$). The LWP adjustments in other seasons exhibit similar diurnal patterns and magnitudes, peaking at noon (black lines in Figures S9F, S11-S12F). This similarity may be due to the weak seasonal variations in the diurnal patterns of LWP and N_d (not shown). The diurnal patterns of warm invigoration in spring and winter are similar to the overall results (blue lines in Figures S9F and S12F compared to Figure 1F). The minimum N_d at 1100 LT coincides with the weakest warm invigoration (i.e., minimal LWP enhancement). Autumn exhibits the lowest N_d among seasons (Figure S11F), corresponding to the weakest warm invigoration ($\sim 50\%/31\%$ lower than spring/winter) and the largest diurnal fluctuations. The diurnal pattern of entrainment feedbacks in spring differs from other seasons, possibly due to its distinct entrainment rate diurnal variation, which can be illustrated by the variation of cloud-top height (CLTH). Here, based on the relationship between CLTH, w_s and w_e ($\frac{dCLTH}{dt} = w_s + w_e$) (Painemal et al., 2013), the diurnal variations of w_e (entrainment rate) can be qualitatively analyzed with the diurnal variations of CLTH and large-scale subsidence (w_s) (Figure S13). Before 1400 LT, the variation of large-scale subsidence is unrelated to CLTH, thus the change in CLTH can only be attributed to entrainment rate. It weakens before 1200 LT, possibly due to the decreasing cloud-top longwave cooling after sunrise. It then increases until 1400 LT which may be caused by the enhanced longwave cooling. After 1400 LT, the decrease in CLTH is caused by the enhancement of large-scale subsidence.”.

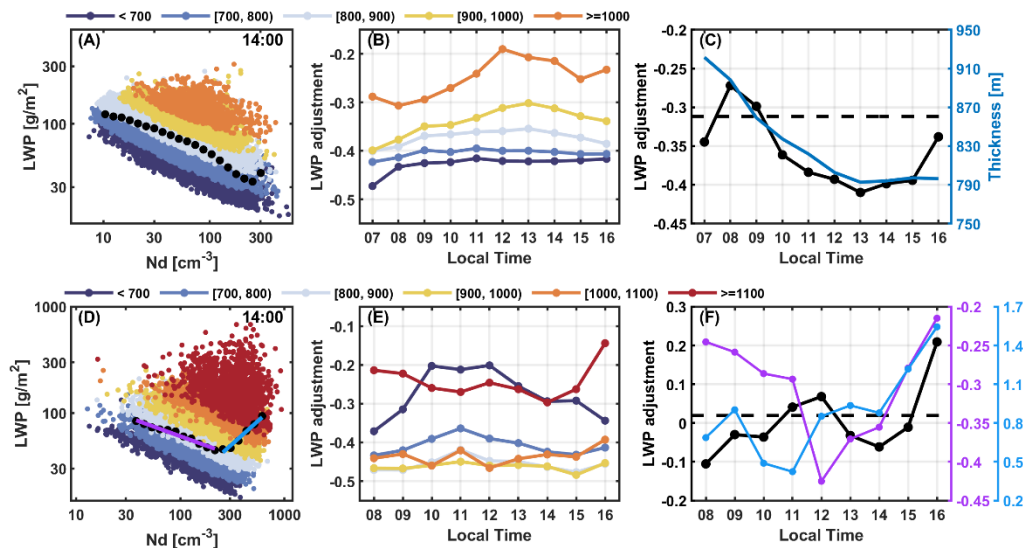


Figure R1. LWP adjustments in log-log spaces and their diurnal patterns in two typical regions (the west of Australia, AUW and the east China sea, ECS). Non-precipitation cloud samples are scattered in N_d -LWP log space at 1400 LT in (A) AUW and (D) ECS region. Colored dots are samples in different cloud thickness (H) bins (unit: m). Black dots represent the median LWP in each N_d bin. The colored lines are the fits of black dots at different stages in ECS region. Diurnal variations of LWP adjustments binned by H in (B) AUW and (E) ECS regions are shown. Colored lines in (F) are diurnal variations of different stages in (D), while black lines in (C) and (F) are the overall diurnal variations of LWP adjustments in two regions, respectively. Blue line in (C) represents the diurnal variation of H. Dashed lines represent the average LWP adjustments considering diurnal variations, -0.31 for AUW (C) and 0.02 for ECS (F). Same as Figure 1 in the revised manuscript.

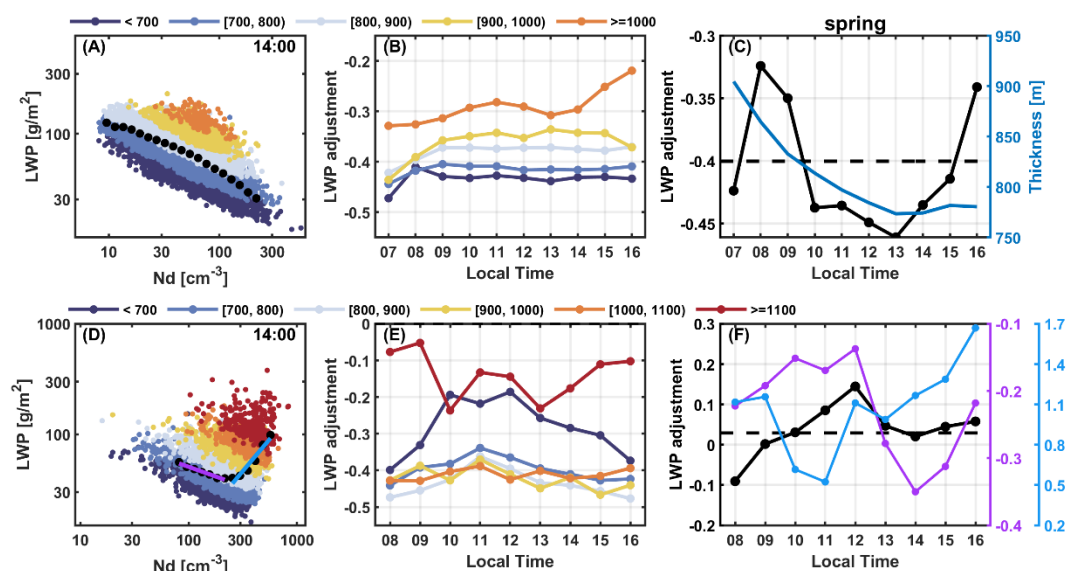


Figure R2. LWP adjustments in log-log spaces and their diurnal patterns in two typical regions (the west of Australia, AUW and the east China sea, ECS) for spring. Same as Figure S9 in the revised Supplementary Materials.

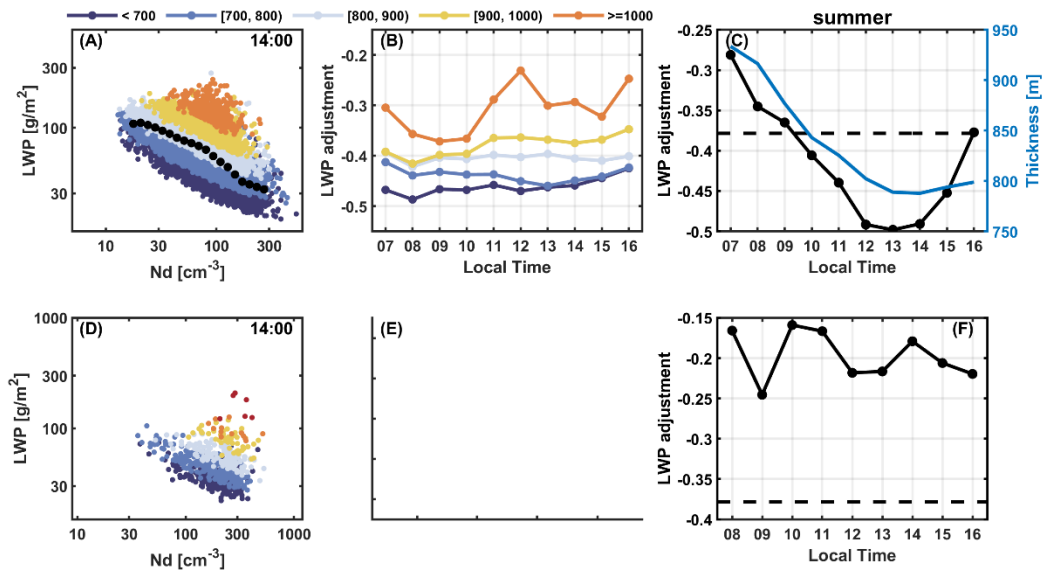


Figure R3. Same as Figure R2 but for summer. The total sample size is 187646 for the AUW region and 5062 for the ECS region. Note that insufficient sample size in the ECS region made LWP adjustment in different H bins impractical, resulting in an empty Figure E. Same as Figure S10 in the revised Supplementary Materials.

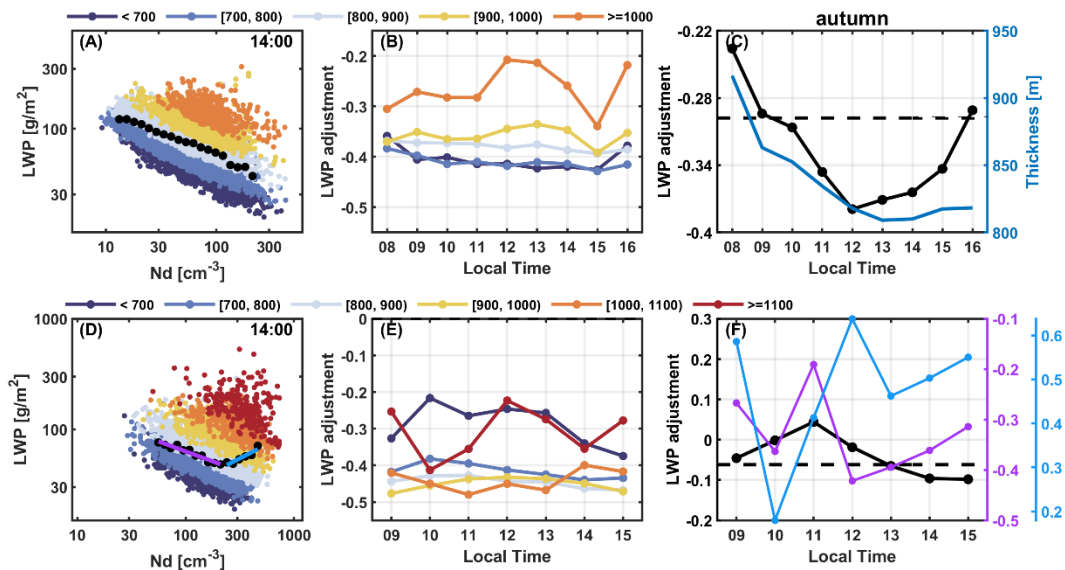


Figure R4. Same as Figure R2 but for autumn. The total sample size was 94311 for the AUW region and 37387 for the ECS region. Same as Figure S11 in the revised Supplementary Materials.

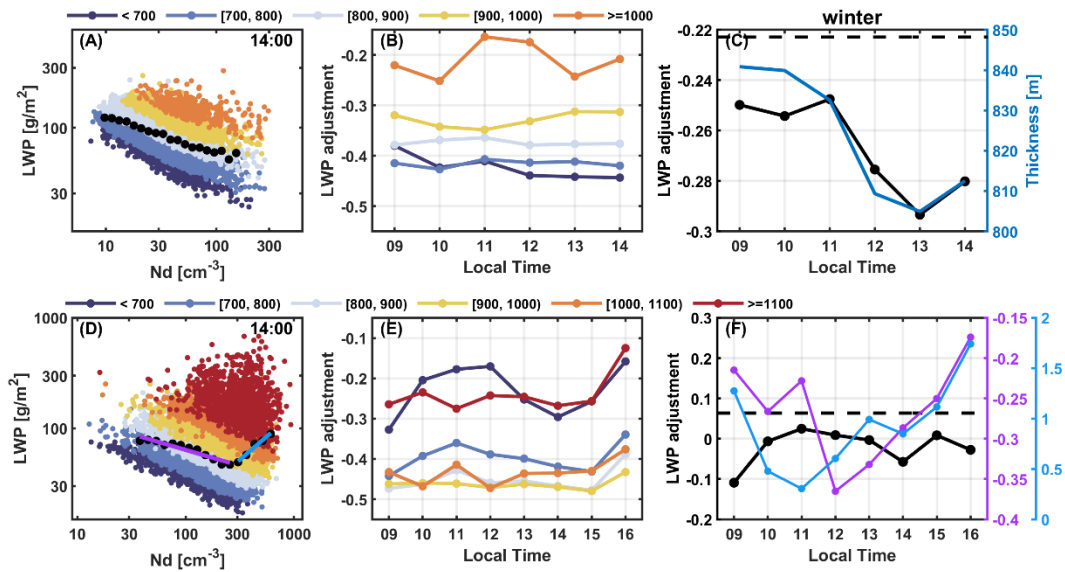


Figure R5. Same as Figure R2 but for winter. The total sample size was 62664 for the AUW region and 76623 for the ECS region. Same as Figure S12 in the revised Supplementary Materials.

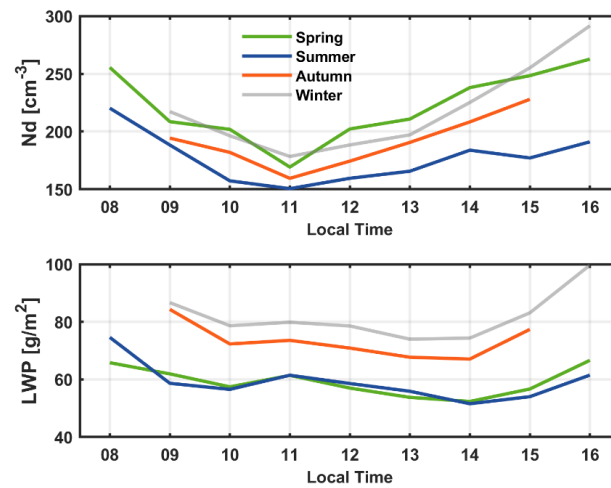


Figure R6. Diurnal variations of N_d and LWP for four seasons in ECS region.

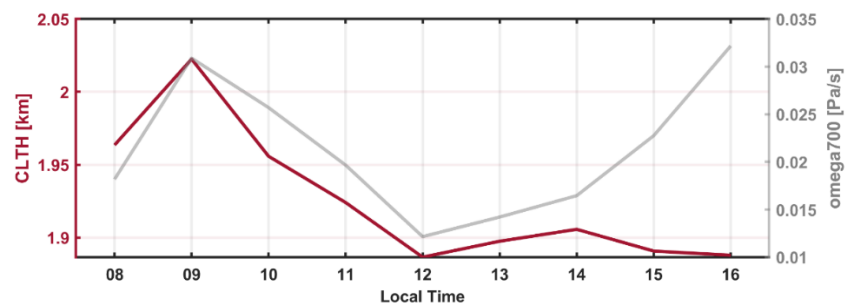


Figure R7. Diurnal variations of cloud-top height (CLTH) and vertical velocity on 700 hPa

(omega700, positive values indicate downdraft) for spring in ECS region. Same as Figure S13 in the revised Supplementary Materials.

2. I am aware of another recent study that examines the diurnal cycle of LWP adjustments over the Eastern North Atlantic (Qiu et al., 2024). The methodology and conceptual framework of that paper are quite similar to the current study, though applied to a different region. Although the authors have cited this work, they have not provided a thorough discussion of it. Given these similarities, I suggest the authors include a discussion comparing their conclusions with those of Qiu et al., 2024, highlighting any key differences or regional contrasts.

Response: Thank you very much for the valuable advice! Our observed diurnal LWP adjustment pattern in the AUW region is consistent with Qiu et al. (2024)'s findings in the eastern North Atlantic, where thick-thin cloud transitions dominated daytime variability. However, while they linked this to regional cloud internal evolution, we identify boundary-layer dynamics (e.g., decoupling and entrainment) as the primary driver. Additionally, the method we used is quite different compared with Qiu et al. (2024). They calculated LWP adjustment within each 1° grid box, assuming constant meteorological conditions, whereas we calculated LWP adjustments with all samples over four years, preserving the influence of meteorological covariations at each moment. By stratifying analyses by cloud thickness according to Rosenfeld et al. (2019), we disentangle meteorological covariations from cloud internal feedbacks. Additionally, cloud thickness remains relatively stable after 1300 LT in our results. The weakening of negative LWP adjustments is primarily due to the weakening of entrainment induced by the strengthening of large-scale subsidence. Therefore, our results tend to emphasize the diurnal variations of LWP adjustments induced by time-dependent meteorological covariations primarily stemming from boundary layer dynamical mechanisms, while Qiu et al. (2024) focused more on the evolution of clouds, suggesting that clouds retain the memory from previous state.

Furthermore, we conduct the same analyses in ECS region with completely different environmental background, and obtain entirely different results. In humid and unstable environments, aerosol-induced warm invigoration is more likely to occur. In this condition, cloud thickness is no longer suitable for distinguishing meteorological conditions as a mediator of N_d -LWP relationship. The cloud thinning mechanism is also insufficient to explain the diurnal variations of LWP adjustments. This demonstrates that the significant regional differences in the diurnal variations of LWP adjustments, depending on

aerosol loadings, cloud regimes and meteorological conditions.

In the revised manuscript, we have included discussion comparing our results with Qiu et al. (2024). The details have been added on Lines 475-482: “Our observed diurnal LWP adjustment pattern in the AUW region is consistent with Qiu et al. (2024)'s findings in the eastern North Atlantic, where thick-thin cloud transitions dominated daytime variability. However, unlike Qiu et al. (2024)'s method, which focused on regional cloud internal evolution and calculated LWP adjustment within each 1° grid box without considering meteorological covariations, this investigation preserves the influence of meteorological covariations at each moment. By stratifying analyses by cloud thickness according to Rosenfeld et al. (2019), we disentangle meteorological covariations from cloud internal feedbacks. Additionally, cloud thickness remains relatively stable after 1300 LT in our results. The weakening of negative LWP adjustments is primarily due to the weakening of entrainment induced by the strengthening of large-scale subsidence.”.

3. Many of the statements in the manuscript appear to be interpretations or inferences drawn from previous studies, rather than conclusions directly supported by the current analysis. However, the authors present these statements as if they are firmly established by their own results. I recommend clarifying which findings are directly derived from the current analysis and distinguishing them from interpretations based on prior work.

Response: Thanks for your suggestion! We apologize for some statements that may mislead the reviewer. We acknowledge that some conclusions could only be inferred based on earlier studies due to the observational limitations, despite our best efforts to use proxies to represent physical processes (such as using LWP skewness to characterize the degree of decoupling). In the revised version, we have further separated the discussion and conclusion sections. Within the conclusion section, the key findings have been further condensed. Please refer to Major comments 5. Throughout the manuscript, any statement about mechanisms derived from previous studies has been carefully rephrased to distinguish the direct conclusions and inferences. For example, some of the revisions on the important parts related to the conclusions are as follows:

The possible mechanisms of diurnal patterns of N_d , r_e and LWP adjustments in AUW region have been rephrased on Lines 344-370: “Unexpectedly, there is no evident diurnal variation of AOD in AUW, but N_d continually declines from 0700 LT to 1600 LT and r_e does not change significantly before 1200 LT and then rises. It is thus reasonable to infer the diurnal variations of N_d and r_e are related with dynamic

process on account of the disagreement with aerosols variations. Combining the nature of decoupling process and diurnal patterns of cloud properties in Figure 6, we discuss the possible mechanisms for the diurnal variation of N_d and r_e based on earlier cloud microphysics studies. According to Verlinden (2018), the shortwave heating counteracts longwave cooling during daytime, resulting in weakening of cloud-top entrainment. Meanwhile, the decoupling that cuts off moisture transport suppresses condensational growth. The combination of these two processes may lead to the little variation in r_e before 1200 LT. Additionally, the decoupling process leads to the suppression of both surface moisture transport and cloud base updrafts, which may in turn reduce the supersaturation and hence the number of activated cloud droplets. This may explain the continuous decrease in N_d before 1300 LT. Furthermore, according to the relationship between CLTH, w_s (always negative) and entrainment rate (w_e) ($\frac{dCLTH}{dt} = w_s + w_e$) in the mixed-layer model framework (Painemal et al., 2013), we explain the variations after 1200 LT. CLTH begins to decrease after 1200 LT, suggesting an intensification of large-scale subsidence (w_s , always negative in Sc region) and/or a weakening of entrainment rate (w_e). Large-scale subsidence on 700 hPa from ERA5 reanalysis becomes stronger (gray line in Figure 6A). It may enhance the temperature-inversion jump, which will in turn decrease the entrainment rate (Painemal et al., 2013). During this period, the condensational growth by the reconstructed water vapor supply will enhance r_e . Meanwhile, the coalescence process, enhanced by an increase in r_e leads to a decrease in N_d . This process could be more dominant than the increase in activated cloud droplets caused by water vapor reestablishment for an increase in N_d to be observed in this study.

Based on the diurnal mechanisms of MBL discussed above, the diurnal pattern of LWP adjustments is primarily a consequence of the influence of these diurnal-related mechanisms on the relationship between N_d and LWP across different microphysical-dynamical conditions. In AUW, the diurnal variations of the overall LWP adjustments (black line in Figure 1C) and cloud thickness (blue line in Figure 1C) demonstrate a strong consistency with a turning point at 1300 LT. The variation of LWP adjustment here is mainly attributed to the gradual thinning of clouds, which reflects the differential LWP responses to N_d with varying H. LWP adjustment becomes more negative with the thinning of cloud, which is consistent with the results in Figure 1B. After 1300 LT, cloud thickness remains almost unchanged. The variation in LWP adjustments is mainly governed the weakening of entrainment due to the intensification of large-scale subsidence (Figure 6A). During this time, the weakening of the

entrainment process leads to a weakening of the negative LWP adjustments over AUW region.”.

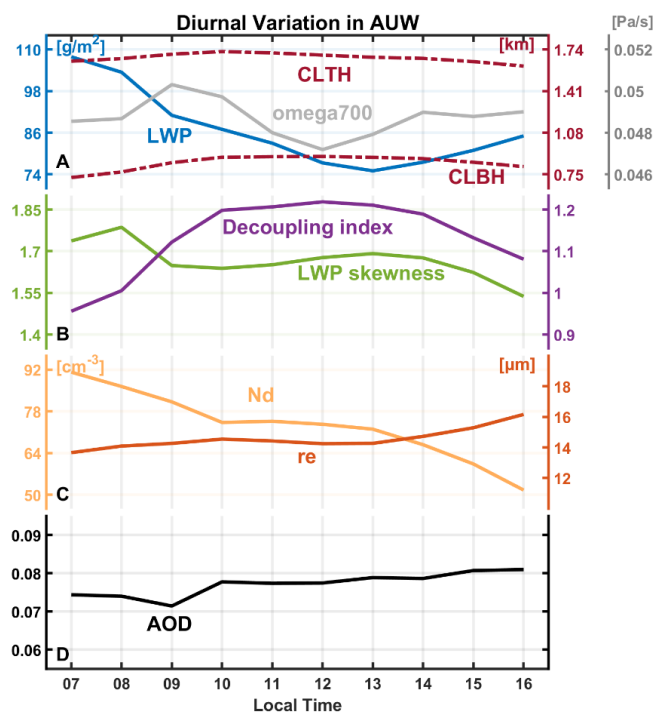


Figure R8. Diurnal patterns in AUW region. (A) Cloud liquid water path (LWP), cloud-top height (CLTH), cloud base height (CLBH) and vertical velocity on 700 hPa (omega700, positive values indicate downdraft) from ERA5 reanalysis. (B) LWP skewness and decoupling index in AUW region. (C) Cloud droplet number concentration (N_d) and effective radius (r_e). (D) Aerosol optical depth (AOD). Same as Figure 6 in the revised manuscript.

The possible mechanisms of diurnal patterns of N_d , r_e and LWP adjustments in ECS region have been rephrased on Lines 396-413: “In terms of microphysical properties, N_d in ECS decreases before 1100 LT and then increases. Variations of r_e are just the opposite except insignificant change since 1400 LT. The crucial mechanism leading to such changes may be attributed to the weakest entrainment drying at 1100 LT, resulting in the highest values of r_e and lowest values of N_d . Such diurnal variations in entrainment have also been observed in other coastal areas. Caldwell et al. (2005) reported the weakest entrainment rate at 1100 LT during East Pacific Investigation of Climate (EPIC) stratocumulus cruise in 2001. Painemal et al. (2017) found the minimum of entrainment occurred between 0900-1100 LT over the northeast Pacific region, attributing the diurnal pattern to the turbulence caused by long-wave radiative cooling. Additionally, other factors may also contribute to the diurnal variations of N_d and r_e . For example, the changes before 1100 LT may include the impacts of reducing aerosol loadings. Subsidence from both

cloud top and bottom occurred after 1400 LT may limit the entrainment and the continuous decline of r_e . Cumulus coupling may also contribute to the increase of N_d , Martin et al. (1995) found local increase in N_d induced by the intrusion of cumulus clouds during ASTEX.

In ECS region, based on the above mechanisms, the diurnal variation of LWP is relatively small, yet N_d exhibits a distinct diurnal pattern. Changes in N_d lead to LWP adjustments that correspond to two microphysical-dynamical processes. The turning point between the two stages exhibits the same diurnal variation as the average N_d (Figure S8). Before noon, a decrease in N_d weakens the warm invigoration (blue line in Figure 1F), while the entrainment feedback intensifies (purple line in Figure 1F). After 1200 LT, the trend reverses. The opposing patterns between warm invigoration and entrainment feedback further reflect their competitive nature. The interaction of these two processes drives the overall diurnal variation in LWP adjustments (black line in Figure 1F).”.

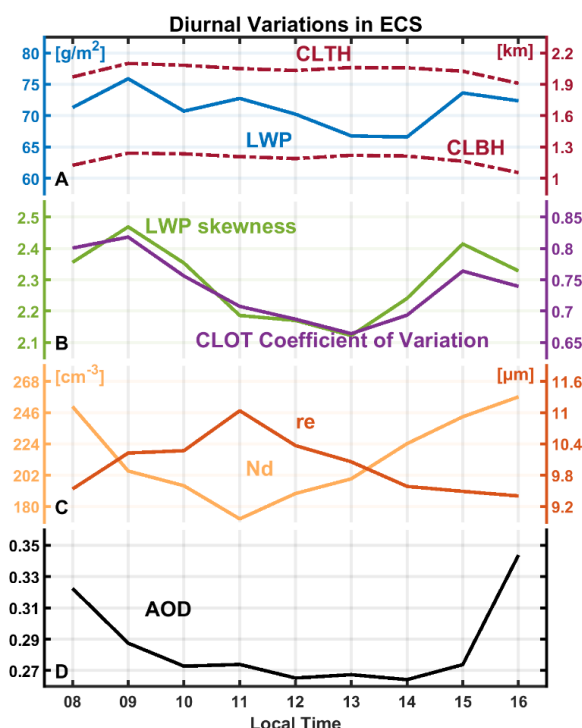


Figure R9. Diurnal patterns in ECS region. (A) Cloud liquid water path (LWP), cloud-top height (CLTH) and cloud base height (CLBH). (B) LWP skewness and coefficient of variation (c_v) of cloud optical depth (CLOT) in AUW region. (C) Cloud droplet number concentration (N_d) and effective radius (r_e). (D) Aerosol optical depth (AOD). Same as Figure 7 in the revised manuscript.

- There are grammatical errors throughout the paper, which occasionally hinder clarity and understanding. I have noted some examples in the minor comments section, but I recommend that

the authors thoroughly proofread the manuscript to address these issues.

Response: We sincerely appreciate the reviewer's feedback about the language in the manuscript. We have carefully revised the manuscript to address these issues and ensure that the language is clear and accurate.

5. While the authors provide a very detailed discussion in the results section, the conclusions at the end of the paper are quite general and lack specificity. Some of these conclusions are too broad to be useful. Instead of simply stating that LWP adjustments depend on microphysical-dynamical processes and meteorological conditions, I recommend that the authors summarize how each condition specifically influences LWP adjustments and what we can learn from them. Presenting the key findings in bullet points would greatly improve clarity and provide a concise summary of the main results.

Response: Thanks for your insightful comments! We agree that the conclusion section is too general. We have separated the discussion and conclusion into two sections, rephrasing a more detailed summary as suggested (see Lines 510-538): “This study reveals the diurnal variations of LWP adjustments in two specific regions within the sight of Himawari-8, along with the possible mechanisms contributing to these variations. The studied regions have significant differences in environmental conditions and aerosol loadings. Although some conclusions are similar to the previous studies, we have also discovered some new phenomena. The observational studies demonstrate LWP adjustments in two regions are determined by the dominant microphysical-dynamical processes in different N_d stages (entrainment feedbacks and warm invigoration), while their diurnal variations depend on the dynamical conditions of the boundary layer. Important findings from this investigation are as follows:

- (1) In AUW region, the diurnal variations of LWP adjustments are insensitive to seasonality. The overall negative LWP adjustments decrease from -0.27 to -0.41 before 1300 LT and then increase to -0.34 . Cloud thickness in AUW region can serve as a confounder to separate the effects of meteorological covariations. The diurnal pattern is primarily associated with cloud thinning induced by decoupling process of MBL quantified by LWP skewness before 1300 LT and the weakening of entrainment induced by intensification of large-scale subsidence after 1300 LT.
- (2) In ECS region, diurnal variations of LWP adjustment exhibit seasonal differences. Samples from winter and spring dominate the overall variations (accounting for 75% of the total

samples). For the overall results, LWP increases and then decreases with N_d , suggesting possible competition between entrainment feedbacks and warm invigoration. The diurnal pattern of LWP adjustments is determined by the combined diurnal variations of these two mechanisms. Warm invigoration is related to the diurnal variation of the N_d at the turning points of the two processes. Lower N_d in the ECS region implies a weaker warm invigoration.

- (3) We indicate an overall underestimation of the cooling effect by LWP adjustment up to 89% (14%), with a further 20% (15%) offset of the Twomey effect when neglecting the diurnal variations of LWP adjustments in AUW (ECS) region. Furthermore, our results quantify the regional impact of boundary layer dynamic conditions on LWP adjustments. For example, diurnal decoupling process in AUW region results in a 219% variation of LWP adjustments within the daytime relative to the daily mean (the diurnal variation range divided by the daily mean), assuming other conditions remain relatively unchanged.

Our research provides a detailed discussion for the diurnal variations of LWP adjustments and how they are influenced by existed boundary layer mechanisms. We underscore the importance of fully considering the covariation with environmental conditions, indicating different potential influencing factors on cloud brightening and radiative forcing in terms of the regional and diurnal daytime scale. It is a highly time-dependent variable lacking quantification and should be taken into consideration of future research in aerosol indirect effects on climate.”.

Minor comments:

1. Line 62: Please check the grammar

Response: Thanks for your careful checks.. We have revised the sentence as (see Lines 60-62): “Our analysis focuses on $1^\circ \times 1^\circ$ non-precipitation marine low-level cloud samples aggregated from filtered pixel-level satellite data. We aim to avoid the impact of precipitation on retrieval of N_d and focus only on the development of clouds in response to aerosol loading associated with microphysical-dynamical conditions over two selected regions.”.

2. Line 73: Why are the retrievals sub-sampled to different resolutions in the Northern and Southern Hemispheres?

Response: Thank you for raising this question! In fact, after consulting the technical staff, we found that the incorrect information on the website had led us to provide inaccurate information in the manuscript

and mislead the reader. We have helped them correct the errors on the website. The observation resolution of CERES_GOES_HIM08 is 2 km at nadir, and has been sub-sampled to 6 km for both the Northern and Southern Hemispheres. The sub-sampled resolution meets the needs of the CERES project without having a data implosion. We have corrected this issue in the revised manuscript on Lines 72-73: “The retrievals are at 2-km resolution (at nadir) and are sub-sampled to 6 km. The sub-sampled resolution meets the needs of the CERES project without having a data implosion.”.

3. Line 75: Could you briefly explain how CLTH, CLBH, and H are retrieved?

Response: Thanks for your comment! CERES_GOES_HIM08 product provides cloud-top height (CLTH), cloud base height (CLBH), and cloud thickness (H) information. They are retrieved based on the CERES Edition 4 (Ed4) cloud property retrieval algorithm system. We have briefly introduced the algorithm of the three parameters on Lines 77-81: “Briefly, CLTH is estimated as the altitude where the cloud-top temperature (CLTT) occurs in the temperature profile. The temperature profile is provided by CERES Meteorology, Ozone, and Aerosol (CERES MOA) dataset. CLTT is derived from an empirical parameterization of cloud-top emissivity at channel 4 and cloud effective temperature. H is computed using empirical formulas with τ : $H = 0.39 \ln \tau - 0.01$ for liquid clouds. CLBH is directly obtained by subtracting H from CLTH.” For specific information, please refer to Minnis et al. (2011, 2021).

4. Lines 80-86: You assume $f_{ad} = 0.8$, which indicates a sub-adiabatic condition. Therefore, the retrieval of N_d is not strictly under the adiabatic assumption (which requires $f_{ad} = 1$). However, LWP appears to be derived assuming adiabatic conditions. This introduces some inconsistency between your N_d and LWP retrievals. Please clarify and address this inconsistency.

Response: Thanks for raising a great point! $LWP = \frac{5}{9} \rho_w \tau r_e$ only highlights its availability for profiles of linearly increasing LWC but does not require the adiabatic assumption (i.e., sub-adiabatic also follow linearly increasing LWC in cloud profile) (Wood and Hartmann, 2006). The relationship is modified by a factor of 0.83 from $\frac{2}{3} \rho_w \tau r_e$ which assumes a vertical homogenous cloud (vertically constant LWC). According to Bennartz (2007), the retrieval method with a factor of 5/9 shows better agreement with microwave observations. Additionally, Lu et al. (2023) have used this method as the actual LWP to estimate the cloud adiabatic fraction with the adiabatic $LWP = \frac{1}{2} c_w H^2$. Therefore, the retrievals of both N_d and LWP are not performed under strictly adiabatic conditions. The combination of these two retrieval methods of N_d and LWP has been widely used in the satellite investigation of LWP adjustment (Fons et

al., 2023; Gryspeerd et al., 2019; Qiu et al., 2023; Smalley et al., 2024).

We apologize for the misleading description, which has been corrected on Lines 83-90: “ N_d can be estimated as (Bennartz, 2007).”:

$$N_d = \frac{\sqrt{5}}{2\pi k} \left(\frac{f_{ad} c_w \tau}{Q \rho_w r_e^5} \right)^{\frac{1}{2}} \quad (1)$$

where τ represents cloud optical depth and ρ_w is liquid water density. The extinction efficiency $Q \approx 2$, as Q relies less on the size parameter in near-infrared. k , related to droplet size distribution, is set as 0.8 for maritime cloud (Martin et al., 1994; Painemal and Zuidema, 2011). c_w represents the condensation rate determined by temperature in cloud (here is cloud-top temperature from SatCORPS). A constant adiabatic value (f_{ad}) of 0.8 is used to represent the deviation from the adiabatic profile (Bennartz, 2007).”, and Lines 94-97: “In this study, the LWP from SatCORPS is calculated as $\frac{5}{9} \rho_w \tau r_e$ in sub-adiabatic conditions, following the method by Wood and Hartmann (2006). The combination of these two retrieval methods of N_d and LWP has been widely used in the satellite investigations of LWP adjustment (Fons et al., 2023; Gryspeerd et al., 2019; Qiu et al., 2023; Smalley et al., 2024).”.

5. Line 93: Why did you choose 268K as the threshold for cloud-top temperature, rather than the more commonly used 273K?

Response: Thank you for your question! The threshold of 273 K is stricter, while 268 K allows for the presence of some supercooled phase, where it is ubiquitous over the Southern Ocean (Hu et al., 2010). Actually, the threshold of 268 K also has been used in previous studies for the threshold of liquid water cloud-top temperature (Bennartz and Rausch (2017), Gryspeerd et al. (2022) and Li et al. (2018)). Our study follows the above studies, and we focus on liquid water clouds, which have typical cloud top temperatures (CLTT) between 268 and 300 K (Bennartz and Rausch, 2017).

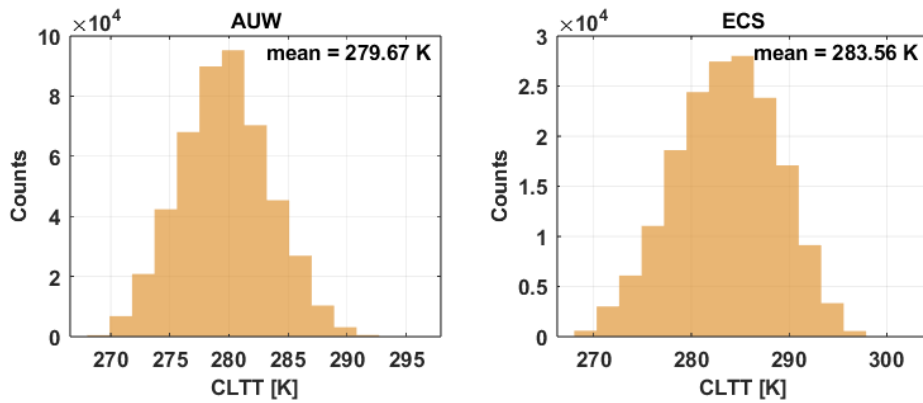


Figure R10. Histogram of cloud-top temperature (CLTT) in AUW (left) and ECS (right) regions.

In addition, we have checked whether this threshold is appropriate. The statistical distributions of CLTT for the samples in this study are presented in Figure R10. Overall, 96% (97%) of the samples are larger than 273 K in AUW (ECS). Therefore, the threshold has a negligible impact on the overall results.

The relevant description has been rephrased to be clearer on Lines 100-103: “To maintain consistency with previous studies (Bennartz and Rausch, 2017; Li et al., 2018), we adopted 268 K as the threshold of CLTT for liquid clouds, rather than 273 K. In fact, 96% (97%) of the samples exhibited CLTT above 273 K in AUW (ECS) region. Therefore, the threshold has a negligible impact on the overall results.”.

6. Line 96: Please check the grammar in this sentence. It should be “Each grid containing at least 30 pixels is considered as a cloud sample.” Additionally, how many pixels are there in total in each $1^\circ \times 1^\circ$ scene?

Response: Thanks for your careful reading. We have corrected the sentence in the revised manuscript. The histograms of samples in $1^\circ \times 1^\circ$ scene are showed in Figure R11 for reviewer’s reference. In total, we collect 480189 $1^\circ \times 1^\circ$ scenes in AUW and 173181 $1^\circ \times 1^\circ$ scenes in ECS. Each scene contains 83 (87) pixels on average in AUW (ECS). We have added the information on Lines 104-105: “Each grid containing at least 30 pixels and is considered as a cloud sample. On average, each grid contains 83 (87) pixels in AUW (ECS) region.”.

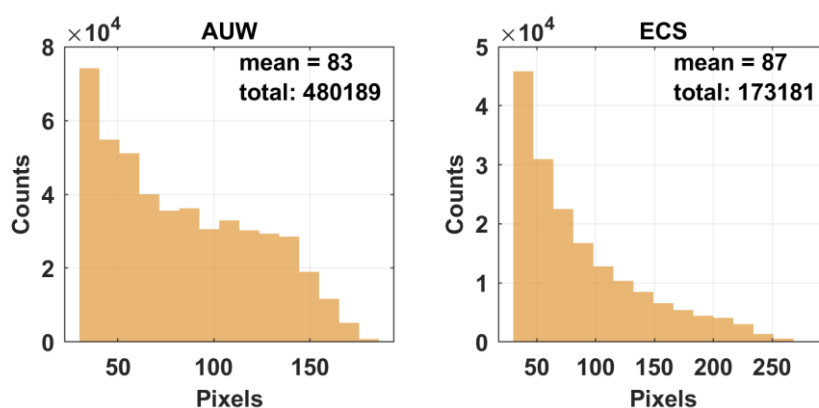


Figure R11. Histograms of pixels in each $1^\circ \times 1^\circ$ scene in AUW (left) and ECS (right) regions.

7. Line 137: Using AOD as a proxy for aerosols introduces uncertainties, as AOD represents column-integrated aerosol loading without indicating aerosol vertical distribution. If aerosols are located above the boundary layer, they may not interact with clouds. However, Figure 8 shows that Nd and AOD are well-correlated, which helps justify using AOD as a proxy. I suggest moving Figure 8 earlier in the manuscript to support the use of AOD.

Response: Thanks for your suggestion. We agree that column AOD is not an adequate proxy. To remain

consistent with earlier studies, we selected AOD as a proxy for aerosols. We have moved the Figure 8 earlier in Figure 5 as suggested. The relevant content has been rephrased to justify the availability of AOD as a proxy (see Lines 253-258): “Note that we select the column AOD as an aerosol proxy to remain consistent with the above studies. Although AOD may not represent aerosol concentrations in some conditions, Figure 5 shows significant correlations observed between the 4-year long-term variations of AOD and N_d at 1200 LT in both regions, particularly in ECS with a correlation of 0.81. Meanwhile, both regions show the similar distribution patterns, with higher N_d and smaller r_e near the continental coastal area, aligning with the average AOD spatial distribution (spatial correlation coefficients of 0.84 in AUW and 0.91 in ECS) (Figure S1), suggesting the availability of AOD as an aerosol proxy.”.

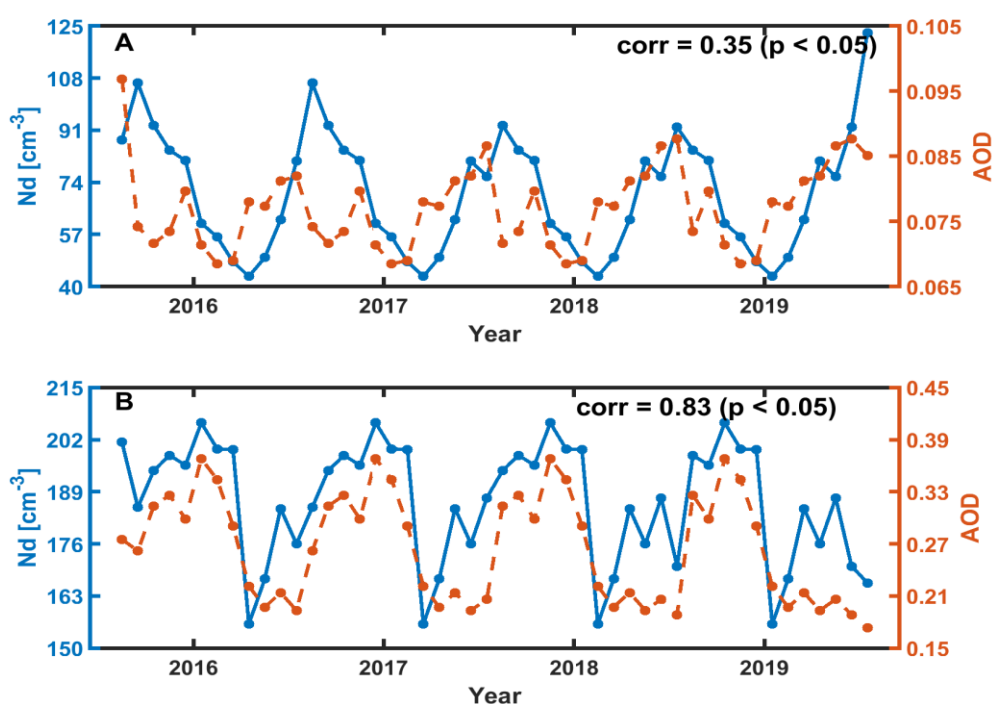


Figure R12. 4-year long-term variations of N_d and total aerosol optical depth (AOD) from MERRA-2 at 1200 LT in AUW (A) and ECS (B) region. The correlation coefficients (corr) between N_d and AOD are 0.35 and 0.83 (significant at the 95% confidence level), respectively. Same as Figure 5 in the revised manuscript.

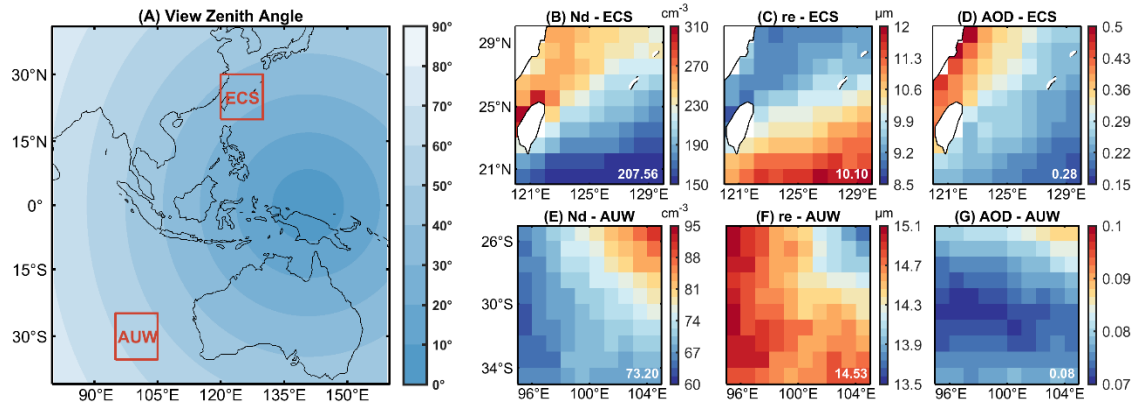


Figure R13. Distributions of cloud properties in two typical regions (the east China sea (20°-30°N, 120°-130°E, ECS) and the west of Australia (25°-35°S, 95°-105°E, AUW). (A) Geographical distribution of the view zenith angle of Satellite Cloud and Radiation Property retrieval System (SatCORPS) Himawari-8 data. The selected regions are marked by red boxes. Spatial distributions of cloud droplet number concentration (N_d) (B, E), effective radius (r_e) (C, F) and total column aerosol optical depth (AOD) (D, G) from MERRA-2 data are presented. The numbers in the lower right corner represent regional averages being weighted by the cosine of latitude. Same as Figure S1 in the revised Supplementary Materials.

8. Line 195. The sentence "These moist and unstable conditions lead..." could benefit from further elaboration. Please clarify how these conditions influence cloud properties.

Response: Thank you for pointing this out. LTS reflects the stability of the boundary layer, influencing the convective property of clouds. Relative humidity (RH) reflects the humidity of free atmosphere, impacting the mixing process at cloud margin and aerosol activations. We have revised the results section and removed the sentence in response to Reviewer #1's comments. However, the descriptions regarding moist and unstable environments remain. And we have provided a detailed account in the revised manuscript according to Reviewer #2's suggestions (Lines 210-217): "Although the microphysical-dynamical processes are challenging to observe directly, environmental conditions can be considered as proxies and provide further support for the invigoration effect. The cloud deepening in ECS region is mainly attributed to increasing CLTH (Figure 2D). Unstable boundary layers (low LTS) favor the formation of more convective clouds (Manshausen et al., 2022), while high RH provides moisture for cloud vertical development. The unstable and moist atmosphere in ECS provides such conditions with a

mean lower-tropospheric stability (LTS) of 15.94 K and a peak in relative humidity on 700 hPa (RH700) of 70% (Figure 3). Gryspeerdt et al. (2019) also reported this rising behavior at high N_d , especially in moist conditions, consistent with our results noted here. Christensen and Stephens (2011) found elevated cloud-top height from open cell clouds in response to ship pollution in relatively unstable and moist conditions.”.

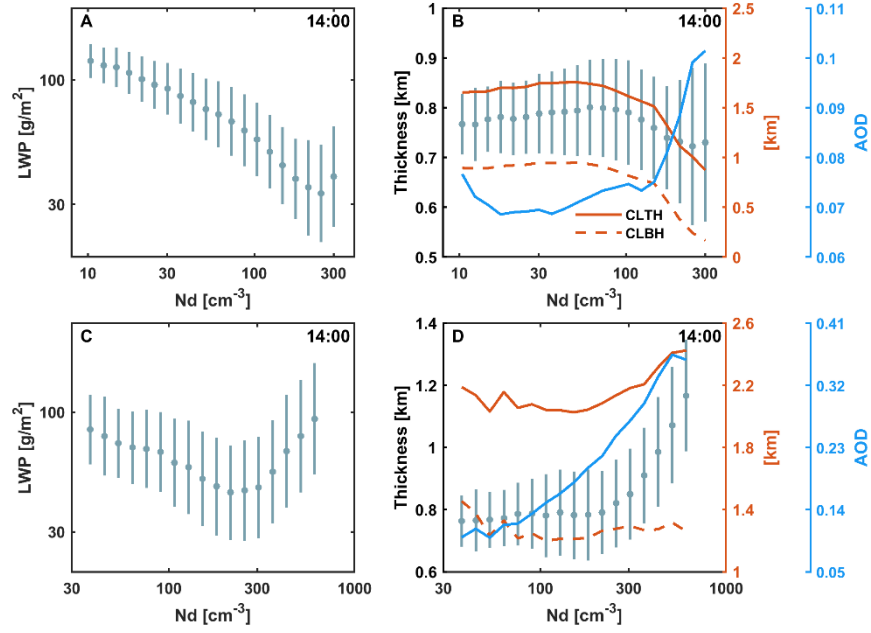


Figure R14. Comparisons between N_d -LWP relationship and N_d -Thickness relationship in two regions. Relationship between N_d and (A) LWP, (B) cloud thickness in AUW region. Relationship between N_d and (C) LWP, (D) cloud thickness in ECS region. The orange solid and dashed lines show the change of cloud top height (CLTH) and cloud base height (CLBH) with N_d . Same as Figure 2 in the revised manuscript.

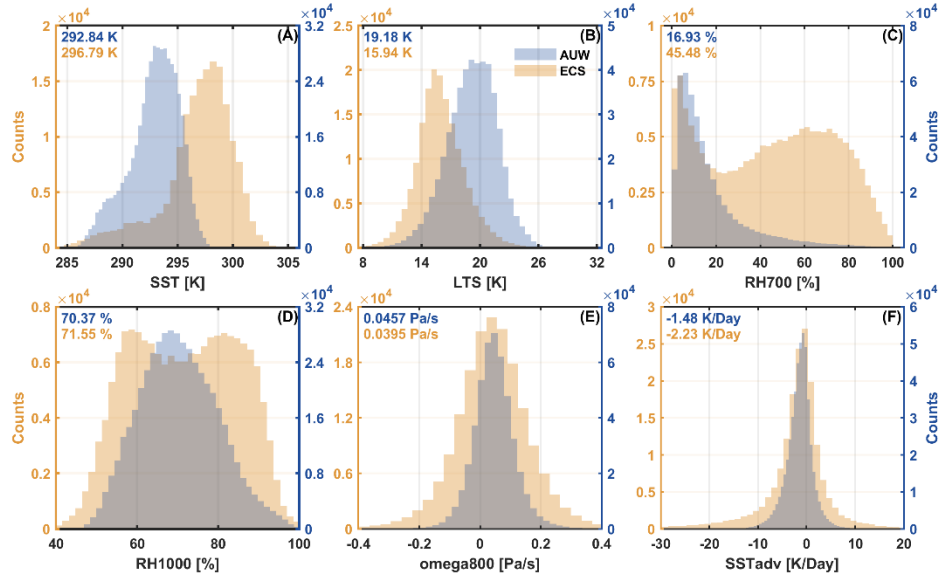


Figure R15. 4-year meteorological conditions of non-precipitation clouds in AUV and ECS regions from 2016 to 2019. Histograms of meteorological factors are presented here. The mean values are labeled in the top-left corner. Data are directly or indirectly derived from ERA5. For vertical velocities on 800 hPa (omega800), positive (negative) values indicate downdraft (updraft). Same as Figure 3 in the revised manuscript.

9. Line 210: The statement "The increasing of LWP at high N_d ..." seems incorrect. It is well-established that increased surface area of cloud droplets can enhance entrainment and evaporation, potentially reducing LWP. Please revise or clarify this point.

Response: Thank you for raising this question! Increased surface area of cloud droplets induced by the increased aerosol loading leads to two opposing effects according to previous studies (Altartaz et al., 2014). On the one hand, they indicated that more droplets delay the collision-coalescence and provide more surface area for condensation, releasing latent heat and promoting cloud vertical development, thus increasing LWP. On the other hand, more small droplets can be more likely to evaporate due to enhanced entrainment, leading to a decreased LWP, as the reviewer mentioned. These two effects determine the final sensitivity of cloud properties (such as cloud depth, LWP, cloud top height) to aerosols in a competitive way, depending on environmental conditions and cloud characteristics (Dagan et al., 2015).

Here in ECS region, our results show that the increasing behavior of LWP at high N_d is consistent with deepening of cloud depth due to increased cloud height. Therefore, we can reasonably infer that this phenomenon represents warm cloud invigoration given the favorable environment conditions in ECS

region. Briefly, high humidity and instability in ECS favor the accumulation of cloud water through condensation. Also, previous studies have reported the occurrence of warm invigoration associated with higher aerosol loading and high proportion of convective clouds(Kaufman et al., 2005; Yuan et al., 2011; Zhang et al., 2021).

We have rephrased the relevant content to be clearer (Lines 189-248): “However, LWP begins to rise at high N_d in ECS (blue line in Figure 1D), which is the primary reason causing the overall positive LWP adjustments in this region. Positive sensitivity over ECS has been reported but not fully understood (Bender et al., 2019; Gryspeerdt et al., 2019; Zhang et al., 2021). Michibata et al. (2016) attributed the positive LWP response in non-precipitation clouds over East Asia to the cloud lifetime effect(Albrecht, 1989). Here in ECS region, clouds are heavily affected by anthropogenic aerosols, showing LWP increases with N_d at high N_d ($>300\text{ cm}^{-3}$). This behavior is related to the deepening of cloud depth with aerosols (Figure 2, C and D), indicating warm invigoration by aerosols (Koren et al., 2014).

The above opposite responses of LWP (either enhanced or decreased) to increasing aerosol loading depends on the environmental conditions and cloud characteristics (Altaratz et al., 2014). On the one hand, they indicated that more droplets delay the collision-coalescence and provide more surface area for condensation, releasing latent heat and promoting cloud vertical development, thus increasing LWP (warm invigoration). On the other hand, more small droplets can be more likely to evaporate due to enhanced entrainment, leading to a decreased LWP (entrainment feedbacks). According to Dagan et al. (2015), the competition between these two processes determines the response of cloud macrophysical properties to aerosols. The N_d -LWP relationship in ECS indicates that warm invigoration takes over after around 300 cm^{-3} leading to cloud deepening. Here, we will demonstrate that ECS region is favorable for warm invigoration to occur from three aspects: environmental conditions, cloud regimes and aerosols.

Although the microphysical-dynamical processes are challenging to observe directly, environmental conditions can be considered as proxies and provide further support for the invigoration effect. The cloud deepening in ECS region is mainly attributed to increasing CLTH (Figure 2D). Unstable boundary layers favor the formation of more convective clouds(Manshausen et al., 2022), while high RH provides moisture for cloud vertical development. The unstable and moist atmosphere in ECS provides such conditions with a mean lower-tropospheric stability (LTS) of 15.94 K and a peak in relative humidity on 700 hPa (RH700) of 70% (Figure 3).Gryspeerdt et al. (2019) also reported this rising behavior at high N_d , especially in moist conditions, consistent with our results noted here. Christensen and Stephens (2011)

found elevated cloud-top height from open cell clouds in response to ship pollution in relatively unstable and moist conditions.

Secondly, the more prevalent convective clouds in the ECS region would be another favorable condition for warm invigoration. Zhang et al. (2021) also attributed the positive LWP adjustments to warm invigoration with the widespread low-level convective clouds (Sc and Cu) in ECS. According to the division from Rosenfeld et al. (2019), we categorize the clouds into three regimes, i.e., Sc ($LTS > 18$ K), Sc to Cu transition ($14\text{ K} \leq LTS \leq 18\text{ K}$), and Cu ($LTS < 14\text{ K}$). (Figure 4, G, H and I). We show that clouds in ECS region are dominated by the Sc to Cu transition regime. The formation of this transition regime is associated with increasing sea surface temperature (SST) due to “deepening-warming decoupling” (Albrecht et al., 1995; Bretherton and Wyant, 1997). Sc presents over the relatively shallow and stable boundary layer with cooler sea surface along the coast (Figure 4, A and B) and most of Sc may be advected from the southeast Chinese plain (Klein and Hartmann, 1993). According to the cloud advection scheme by Miller et al. (2018), cloud advection can be approximated as a translation of the cloud field with the wind field. The advection height is assumed to correspond to the height of the cloud top. Therefore, we can simply deduce from the wind field on 700 hPa (Figure 4A) that clouds in ECS have the possibility of advection from the Chinese plain in the west. As air moves offshore, MBL deepens and cloud layer decouples with the surface mixed layer over the warmer sea surface. Cu forms in the moist and unstable subcloud layer and rises to the upper cloud layer, resulting in a local cumulus-coupled MBL.

Finally, at high aerosol-loading conditions, warm invigoration has been found in numerous studies. For instance, Kaufman et al. (2005) reported larger LWP in higher aerosol loading conditions over Atlantic warm clouds (a mix of stratus and trade cumulus) using MODIS observations. Yuan et al. (2011) found increased cloud amount and higher cloud top heights associated with volcanic aerosols in trade cumulus near Hawaii with A-Train satellites. In contrast to the model results of Koren et al. (2014), who suggested that warm invigoration saturates at higher aerosol loading ($AOD \sim 0.3$), our findings indicate a higher AOD of 0.41 (Figure 2), which is reasonable because the saturation value of AOD exhibits regional variability. For example, Kaufman et al. (2005) reported a maximum AOD of 0.46, while Zhang et al. (2021) found that the AOD in the ECS region is approximately 0.4. To summarize, these evidences all confirm the plausibility of warm invigoration in the ECS region, causing the positive LWP adjustments at high N_d .”.

10. Line 214: Please define the "invigoration effect" clearly when first mentioned.

Response: Thanks! We have added a detailed explanation of the invigoration effect in the revised manuscript on Lines 195-199: "The above opposite responses of LWP (either enhanced or decreased) to increasing aerosol loading depends on the environmental conditions and cloud characteristics (Altartatz et al., 2014). On the one hand, they indicated that more droplets delay the collision-coalescence and provide more surface area for condensation, releasing latent heat and promoting cloud vertical development, thus increasing LWP (warm invigoration). On the other hand, more small droplets can be more likely to evaporate due to enhanced entrainment, leading to a decreased LWP (entrainment feedbacks).".

11. Line 244: Replace makes with make.

Response: Thank you for your careful review. The mistake has been corrected in the revised version.

12. Line 251: The statement "we find that LWP adjustments become negative" is incomplete. Please specify whether this refers to high or low cloud thickness (H).

Response: Sorry for the misleading. This sentence means that when we calculated LWP adjustments using mixing samples with different H, LWP adjustments present both positive and negative conditions. However, when we calculated in specific H bins, it becomes all negative. We have rephrased it in the revised version to be clearer on Lines 278-279: "However, we find that LWP adjustments become negative after constraining H in the intervals of Figure 1 (B and E), indicating the dominant effect of entrainment processes.".

13. Fig. 4. I recommend adding the wind field to one of the panels in Figure 4 instead of showing it separately in Figure S6.

Response: Thanks for your suggestion! As shown in Figure R16, we have added the wind field in Figure 4 in the revised manuscript.

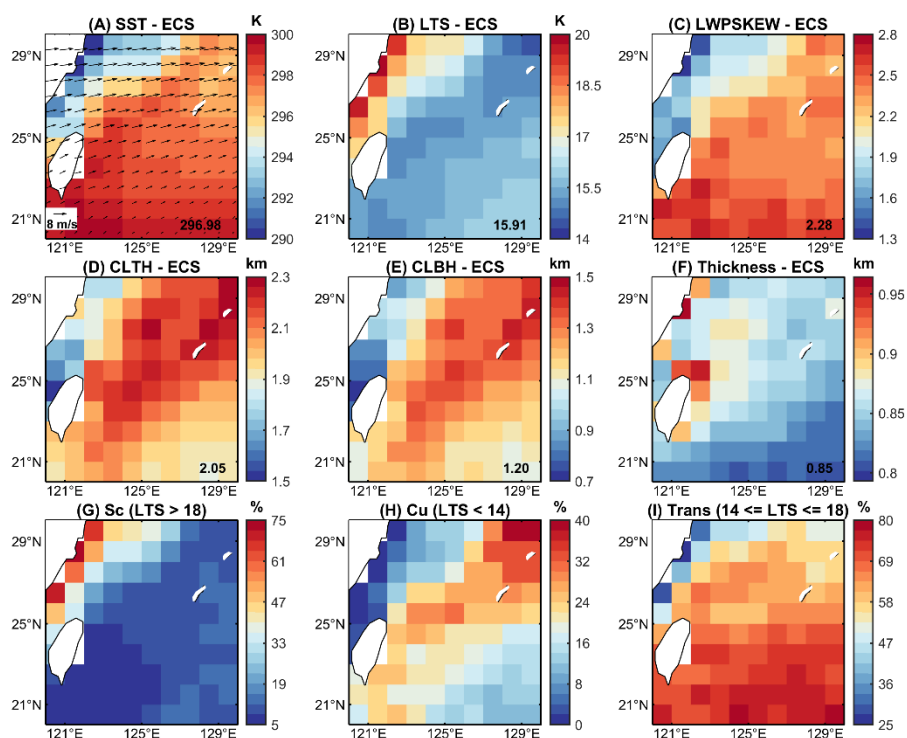


Figure R16. Modified Figure 4 for the revised manuscript.

14. Line 262. “This indicates that clouds of different H respond differently to entrainment”. This is a known fact, but the authors write it in a way that makes it seem like a new finding.

Response: We sincerely appreciate the reviewer’s suggestion. This statement is indeed misleading. We have deleted the statement in the revised manuscript to ensure clarity and accuracy.

15. Lines 272-277. This summary is too general. Instead, please explicitly summarize how LWP adjustments are influenced by specific environmental factors such as LTS, cloud thickness (H), etc.

Response: We are grateful for your suggestion. We have added more investigations of impact of the environmental factors on LWP adjustment in the revised manuscript on Lines 265-273. And we have rephrased the summary section to be more specific on Lines 293-298.

Lines 265-273: “We further analyze the influence of meteorological conditions (i.e., LTS and RH) on LWP adjustments in the two regions (Figure S7). Overall, LWP adjustments cannot be explained by a single meteorological factor. For example, in ECS region, despite the similarity in diurnal patterns of LWP adjustment within different LTS bins, the magnitudes exhibit significant differences due to different aerosol loadings. Samples with $LTS > 18$ K are concentrated in coastal areas with higher aerosol loadings. Warm invigoration is stronger for these samples, thus the overall LWP adjustment is positive. In contrast, samples with $LTS < 18$ K have a larger proportion of smaller aerosol loadings. The effect of

entrainment feedback is more pronounced. This further highlights the importance of aerosol loadings in regulating LWP adjustments in ECS region. Meanwhile, the intricate interplay among meteorological factors, clouds, and aerosols makes it difficult to exclude the influences from meteorological factors (Chen et al., 2014; Engström and Ekman, 2010; Zhang and Feingold, 2023).”.

Lines 293-298: “In summary, the above results indicate that LWP adjustments depend on entrainment feedbacks with increasing N_d in AUW region. While in ECS region, LWP adjustments are results of the competition between entrainment feedbacks and warm invigoration. Given that LWP adjustment is influenced by a complex interaction of meteorological factors, we think that cloud conditions provide more reliable indications. Specifically, cloud thickness is important in AUW region, whereas aerosol loading (represented by N_d) is a better indicator in the ECS region. Therefore, the diurnal variations of these factors can provide important indications for us to investigate the potential mechanisms driving diurnal variations of LWP adjustments.”.

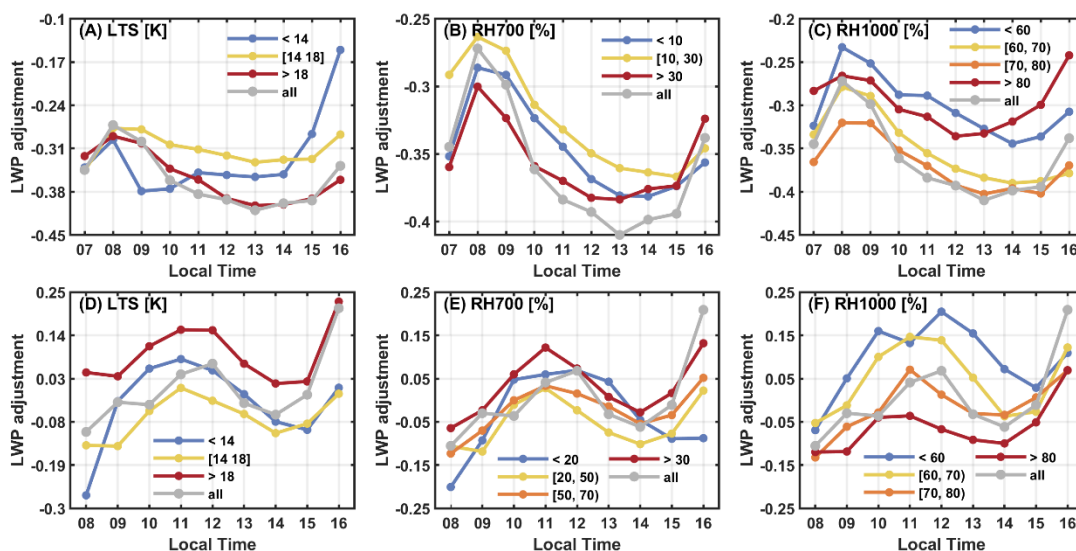


Figure R17. Diurnal patterns of LWP adjustments within different bins of meteorological factors (lower-tropospheric stability (LTS), relative humidity on 700 hPa and 1000 hPa (RH700 and RH1000)). The top row shows results for AUW region, and the bottom row shows results for ECS region. Due to sample size limitations, LWP adjustment at each point is the regression slope of N_d and LWP in log-log space for all samples at that condition. Same as Figure S7 in the revised Supplementary Materials.

16. Lines 314-315. The phrase “illustrating the decoupling process ...” needs further explanation. Please expand.

Response: Thanks for your comments. We use LWP skewness as the quantification of decoupling degree. As the formation of Cu beneath Sc causes positive skewness of probability density function (PDF) of LWP of Sc decks during cold advection (Zheng et al., 2018). We have added further explanation for the LWP skewness in the revised manuscript (Lines 333-334): “Positive skewness indicates more data tends to be distributed to the right, and vice versa. Larger LWP skewness indicates a larger decoupling degree.”.

17. Line 330. You mention w_s (large-scale subsidence), but I don't believe this quantity is directly observable from your dataset. Please clarify.

Response: Thanks for your comment! Here we try to speculate the change of entrainment rate according to the change of CLTH based on Painemal et al. (2013). After 1200 LT, CLTH decreases, which means $\frac{dCLTH}{dt}$ becomes negative. According to the formula $\frac{dCLTH}{dt} = w_s + w_e$, negative $\frac{dCLTH}{dt}$ is subject to decreasing w_s and/or decreasing w_e (entrainment rate). w_s is always negative in Sc region and decreasing w_s refers to enhancing subsidence which will in turn decrease w_e . Therefore, negative $\frac{dCLTH}{dt}$ can always lead to decrease of w_e .

To ensure the completeness of the inference, we have supplemented the diurnal variation of large-scale vertical velocity on 700 hPa based on ERA5 reanalysis in Figure R8 and Figure 6 in the revised manuscript. After 1200 LT, enhancement of large-scale subsidence is presented (positive values indicate downdraft, unit Pa/s). We have rephrased the relevant description to further confirm the credibility of our result (Lines 353-358): “Furthermore, according to the relationship between CLTH, w_s (always negative) and entrainment rate (w_e) ($\frac{dCLTH}{dt} = w_s + w_e$) in the mixed-layer model framework (Painemal et al., 2013), we explain the variations after 1200 LT. CLTH begins to decrease after 1200 LT, suggesting an intensification of large-scale subsidence (w_s , always negative in Sc region) and/or a weakening of entrainment rate (w_e). Large-scale subsidence on 700 hPa from ERA5 reanalysis becomes stronger (gray line in Figure 6A). It may enhance the temperature-inversion jump, which will in turn decrease the entrainment rate (Painemal et al., 2013).”.

18. Line 336. You mention "the diurnal pattern of LWP." Could you indicate clearly where this is shown (e.g., in Figure 1)?

Response: Thanks for your comment! In Figure 1, we primarily discuss the diurnal variations of the LWP adjustments. Please refer to Figure 6 for the diurnal variation of LWP.

19. Line 341. The sentence "cloud-top entrainment weakens, as discussed earlier" is difficult to follow.

I recommend reorganizing this section so that the evidence and conclusion are more closely connected and easy to trace.

Response: Thanks for your valuable feedback! We apologize for any confusion it may have caused. According to Reviewer #1's comment, we have revised the section about the mechanisms governing the diurnal variation of LWP adjustments in AUW region. We also ensured that the description of our conclusions is easy to follow. This section has been accordingly rephrased as follows (Lines 362-370):

“Based on the diurnal mechanisms of MBL discussed above, the diurnal pattern of LWP adjustments is primarily a consequence of the influence of these diurnal-related mechanisms on the relationship between N_d and LWP across different microphysical-dynamical conditions. In AUW, the diurnal variations of the overall LWP adjustments (black line in Figure 1C) and cloud thickness (blue line in Figure 1C) demonstrate a strong consistency with a turning point at 1300 LT. The variation of LWP adjustment here is mainly attributed to the gradual thinning of clouds, which reflects the differential LWP responses to N_d with varying H. LWP adjustment becomes more negative with the thinning of cloud, which is consistent with the results in Figure 1B. After 1300 LT, cloud thickness remains almost unchanged. The variation in LWP adjustments is mainly governed the weakening of entrainment due to the intensification of large-scale subsidence (Figure 6A). During this time, the weakening of the entrainment process leads to a weakening of the negative LWP adjustments over AUW region.”.

20. Line 367. You state, "the strongest stability of the transition layer occurs at 1300 LT." How is this determined from your data? Please clarify.

Response: Thanks for your comment! Since the transition layer is a thin layer above the subcloud layer, it is challenging to observe it through satellite or to capture it with reanalysis data. In fact, this mechanism is mentioned to explain the diurnal variation of LWP skewness in ECS region. Clouds in ECS region is governed by transition regime. We used LWP skewness to indicate cumulus activity in our manuscript, which exhibits a significant diurnal variation. Miller et al. (1998) and Rogers et al. (1995) indicated that the cumulus activity in the transition region is determined by the stability of the transition layer. So we applied the theory of cumulus activity with respect to the transition layer stability proposed by to explain the diurnal variation of LWP skewness.

We have revised this section to clarify the descriptions, ensuring that speculation is clearly distinguished from the main conclusions of the paper (Lines 389-395): “In the ECS region, the weakest cumulus activity occurs at 1300 LT (the lowest LWP skewness in Figure 7B), which may be attributed

to solar insolation. In the Sc to Cu transition region, the decoupled cloud layer and subcloud layer are often separated by a stable transition layer, which has been widely observed by the Atlantic Stratocumulus Transition Experiment (ASTEX) conducted over the northeast Atlantic Ocean. Based on ASTEX, Rogers et al. (1995) suggested that the shortwave radiation would hinder convection during daytime by increasing the stability of the transition layer. Miller et al. (1998) extended this theory to the diurnal variations and believed that the diurnal variation of Cu development was regulated by the stability of the transition layer.”.

Reference:

- Albrecht, B. A.: Aerosols, Cloud Microphysics, and Fractional Cloudiness, *Science*, 245, 1227–1230, <https://doi.org/10.1126/science.245.4923.1227>, 1989.
- Albrecht, B. A., Bretherton, C. S., Johnson, D., Scubert, W. H., and Frisch, A. S.: The Atlantic Stratocumulus Transition Experiment—ASTEX, *Bulletin of the American Meteorological Society*, 76, 889–904, [https://doi.org/10.1175/1520-0477\(1995\)076<0889:TASTE>2.0.CO;2](https://doi.org/10.1175/1520-0477(1995)076<0889:TASTE>2.0.CO;2), 1995.
- Altaratz, O., Koren, I., Remer, L. A., and Hirsch, E.: Review: Cloud invigoration by aerosols—Coupling between microphysics and dynamics, *Atmospheric Research*, 140–141, 38–60, <https://doi.org/10.1016/j.atmosres.2014.01.009>, 2014.
- Bender, F. A.-M., Frey, L., McCoy, D. T., Grosvenor, D. P., and Mohrmann, J. K.: Assessment of aerosol–cloud–radiation correlations in satellite observations, climate models and reanalysis, *Clim Dyn*, 52, 4371–4392, <https://doi.org/10.1007/s00382-018-4384-z>, 2019.
- Bennartz, R.: Global assessment of marine boundary layer cloud droplet number concentration from satellite, *J. Geophys. Res.*, 112, D02201, <https://doi.org/10.1029/2006JD007547>, 2007.
- Bennartz, R. and Rausch, J.: Global and regional estimates of warm cloud droplet number concentration based on 13 years of AQUA-MODIS observations, *Atmos. Chem. Phys.*, 17, 9815–9836, <https://doi.org/10.5194/acp-17-9815-2017>, 2017.
- Bretherton, C. S. and Wyant, M. C.: Moisture Transport, Lower-Tropospheric Stability, and Decoupling of Cloud-Topped Boundary Layers, *Journal of the Atmospheric Sciences*, 54, 148–167, [https://doi.org/10.1175/1520-0469\(1997\)054<0148:MTL TSA>2.0.CO;2](https://doi.org/10.1175/1520-0469(1997)054<0148:MTL TSA>2.0.CO;2), 1997.
- Caldwell, P., Bretherton, C. S., and Wood, R.: Mixed-Layer Budget Analysis of the Diurnal Cycle of Entrainment in Southeast Pacific Stratocumulus, *Journal of the Atmospheric Sciences*, 62, 3775–3791, <https://doi.org/10.1175/JAS3561.1>, 2005.
- Chen, Y.-C., Christensen, M. W., Stephens, G. L., and Seinfeld, J. H.: Satellite-based estimate of global aerosol–cloud radiative forcing by marine warm clouds, *Nature Geosci*, 7, 643–646, <https://doi.org/10.1038/ngeo2214>, 2014.
- Christensen, M. W. and Stephens, G. L.: Microphysical and macrophysical responses of marine stratocumulus polluted by underlying ships: Evidence of cloud deepening, *J. Geophys. Res.*, 116, D03201, <https://doi.org/10.1029/2010JD014638>, 2011.
- Dagan, G., Koren, I., and Altaratz, O.: Competition between core and periphery-based processes in warm convective clouds – from invigoration to suppression, *Atmospheric Chemistry and Physics*, 15, 2749–2760, <https://doi.org/10.5194/acp-15-2749-2015>, 2015.

Engström, A. and Ekman, A. M. L.: Impact of meteorological factors on the correlation between aerosol optical depth and cloud fraction: IMPACTS ON AEROSOL-CLOUD RELATIONSHIPS, *Geophys. Res. Lett.*, 37, n/a-n/a, <https://doi.org/10.1029/2010GL044361>, 2010.

Fons, E., Runge, J., Neubauer, D., and Lohmann, U.: Stratocumulus adjustments to aerosol perturbations disentangled with a causal approach, *npj Clim Atmos Sci*, 6, 130, <https://doi.org/10.1038/s41612-023-00452-w>, 2023.

Gryspeerdt, E., Goren, T., Sourdeval, O., Quaas, J., Mülmenstädt, J., Dipu, S., Unglaub, C., Gettelman, A., and Christensen, M.: Constraining the aerosol influence on cloud liquid water path, *Atmos. Chem. Phys.*, 19, 5331–5347, <https://doi.org/10.5194/acp-19-5331-2019>, 2019.

Gryspeerdt, E., McCoy, D. T., Crosbie, E., Moore, R. H., Nott, G. J., Painemal, D., Small-Griswold, J., Sorooshian, A., and Ziemba, L.: The impact of sampling strategy on the cloud droplet number concentration estimated from satellite data, *Atmos. Meas. Tech.*, 15, 3875–3892, <https://doi.org/10.5194/amt-15-3875-2022>, 2022.

Hu, Y., Rodier, S., Xu, K., Sun, W., Huang, J., Lin, B., Zhai, P., and Josset, D.: Occurrence, liquid water content, and fraction of supercooled water clouds from combined CALIOP/IIR/MODIS measurements, *Journal of Geophysical Research: Atmospheres*, 115, <https://doi.org/10.1029/2009JD012384>, 2010.

Kaufman, Y. J., Koren, I., Remer, L. A., Rosenfeld, D., and Rudich, Y.: The effect of smoke, dust, and pollution aerosol on shallow cloud development over the Atlantic Ocean, *Proc. Natl. Acad. Sci. U.S.A.*, 102, 11207–11212, <https://doi.org/10.1073/pnas.0505191102>, 2005.

Klein, S. A. and Hartmann, D. L.: The Seasonal Cycle of Low Stratiform Clouds, *Journal of Climate*, 6, 1587–1606, [https://doi.org/10.1175/1520-0442\(1993\)006<1587:TSCOLS>2.0.CO;2](https://doi.org/10.1175/1520-0442(1993)006<1587:TSCOLS>2.0.CO;2), 1993.

Koren, I., Dagan, G., and Altaratz, O.: From aerosol-limited to invigoration of warm convective clouds, *Science*, 344, 1143–1146, <https://doi.org/10.1126/science.1252595>, 2014.

Li, J., Jian, B., Huang, J., Hu, Y., Zhao, C., Kawamoto, K., Liao, S., and Wu, M.: Long-term variation of cloud droplet number concentrations from space-based Lidar, *Remote Sensing of Environment*, 213, 144–161, <https://doi.org/10.1016/j.rse.2018.05.011>, 2018.

Lu, X., Mao, F., Rosenfeld, D., Zhu, Y., Zang, L., Pan, Z., and Gong, W.: The Temperature Control of Cloud Adiabatic Fraction and Coverage, *Geophysical Research Letters*, 50, e2023GL105831, <https://doi.org/10.1029/2023GL105831>, 2023.

Manshausen, P., Watson-Parris, D., Christensen, M. W., Jalkanen, J.-P., and Stier, P.: Invisible ship tracks show large cloud sensitivity to aerosol, *Nature*, 610, 101–106, <https://doi.org/10.1038/s41586-022-05122-0>, 2022.

Martin, G. M., Johnson, D. W., and Spice, A.: The Measurement and Parameterization of Effective Radius of Droplets in Warm Stratocumulus Clouds, *Journal of the Atmospheric Sciences*, 51, 1823–1842, [https://doi.org/10.1175/1520-0469\(1994\)051<1823:TMAPOE>2.0.CO;2](https://doi.org/10.1175/1520-0469(1994)051<1823:TMAPOE>2.0.CO;2), 1994.

Martin, G. M., Johnson, D. W., Rogers, D. P., Jonas, P. R., Minnis, P., and Hegg, D. A.: Observations of the Interaction between Cumulus Clouds and Warm Stratocumulus Clouds in the Marine Boundary Layer during ASTEX, *Journal of the Atmospheric Sciences*, 52, 2902–2922, [https://doi.org/10.1175/1520-0469\(1995\)052<2902:OOTIBC>2.0.CO;2](https://doi.org/10.1175/1520-0469(1995)052<2902:OOTIBC>2.0.CO;2), 1995.

Michibata, T., Suzuki, K., Sato, Y., and Takemura, T.: The source of discrepancies in aerosol–cloud–precipitation interactions between GCM and A-Train retrievals, *Atmos. Chem. Phys.*, 16, 15413–15424, <https://doi.org/10.5194/acp-16-15413-2016>, 2016.

Miller, M. A., Jensen, M. P., and Clothiaux, E. E.: Diurnal Cloud and Thermodynamic Variations in the Stratocumulus Transition Regime: A Case Study Using In Situ and Remote Sensors, *Journal of the*

Atmospheric Sciences, 55, 2294–2310, [https://doi.org/10.1175/1520-0469\(1998\)055<2294:DCATVI>2.0.CO;2](https://doi.org/10.1175/1520-0469(1998)055<2294:DCATVI>2.0.CO;2), 1998.

Miller, S. D., Rogers, M. A., Haynes, J. M., Sengupta, M., and Heidinger, A. K.: Short-term solar irradiance forecasting via satellite/model coupling, *Solar Energy*, 168, 102–117, <https://doi.org/10.1016/j.solener.2017.11.049>, 2018.

Minnis, P., Sun-Mack, S., Young, D. F., Heck, P. W., Garber, D. P., Chen, Y., Spangenberg, D. A., Arduini, R. F., Trepte, Q. Z., Smith, W. L., Ayers, J. K., Gibson, S. C., Miller, W. F., Hong, G., Chakrapani, V., Takano, Y., Liou, K.-N., Xie, Y., and Yang, P.: CERES Edition-2 Cloud Property Retrievals Using TRMM VIRS and Terra and Aqua MODIS Data—Part I: Algorithms, *IEEE Trans. Geosci. Remote Sensing*, 49, 4374–4400, <https://doi.org/10.1109/TGRS.2011.2144601>, 2011.

Minnis, P., Sun-Mack, S., Chen, Y., Chang, F.-L., Yost, C. R., Smith, W. L., Heck, P. W., Arduini, R. F., Bedka, S. T., Yi, Y., Hong, G., Jin, Z., Painemal, D., Palikonda, R., Scarino, B. R., Spangenberg, D. A., Smith, R. A., Trepte, Q. Z., Yang, P., and Xie, Y.: CERES MODIS Cloud Product Retrievals for Edition 4—Part I: Algorithm Changes, *IEEE Transactions on Geoscience and Remote Sensing*, 59, 2744–2780, <https://doi.org/10.1109/TGRS.2020.3008866>, 2021.

Painemal, D. and Zuidema, P.: Assessment of MODIS cloud effective radius and optical thickness retrievals over the Southeast Pacific with VOCALS-REx in situ measurements, *Journal of Geophysical Research: Atmospheres*, 116, <https://doi.org/10.1029/2011JD016155>, 2011.

Painemal, D., Minnis, P., and O’Neill, L.: The Diurnal Cycle of Cloud-Top Height and Cloud Cover over the Southeastern Pacific as Observed by GOES-10, *Journal of the Atmospheric Sciences*, 70, 2393–2408, <https://doi.org/10.1175/JAS-D-12-0325.1>, 2013.

Painemal, D., Xu, K., Palikonda, R., and Minnis, P.: Entrainment rate diurnal cycle in marine stratiform clouds estimated from geostationary satellite retrievals and a meteorological forecast model, *Geophysical Research Letters*, 44, 7482–7489, <https://doi.org/10.1002/2017GL074481>, 2017.

Qiu, S., Zheng, X., Painemal, D., Terai, C., and Zhou, X.: Diurnal variation of aerosol indirect effect for warm marine boundary layer clouds in the eastern north Atlantic, *Clouds and Precipitation/Remote Sensing/Troposphere/Physics (physical properties and processes)*, <https://doi.org/10.5194/egusphere-2023-1676>, 2023.

Qiu, S., Zheng, X., Painemal, D., Terai, C. R., and Zhou, X.: Daytime variation in the aerosol indirect effect for warm marine boundary layer clouds in the eastern North Atlantic, *Atmospheric Chemistry and Physics*, 24, 2913–2935, <https://doi.org/10.5194/acp-24-2913-2024>, 2024.

Rogers, D. P., Yang, X., Norris, P. M., Johnson, D. W., Martin, G. M., Friehe, C. A., and Berger, B. W.: Diurnal Evolution of the Cloud-Topped Marine Boundary Layer. Part I: Nocturnal Stratocumulus Development, *Journal of the Atmospheric Sciences*, 52, 2953–2966, [https://doi.org/10.1175/1520-0469\(1995\)052<2953:DEOTCT>2.0.CO;2](https://doi.org/10.1175/1520-0469(1995)052<2953:DEOTCT>2.0.CO;2), 1995.

Rosenfeld, D., Zhu, Y., Wang, M., Zheng, Y., Goren, T., and Yu, S.: Aerosol-driven droplet concentrations dominate coverage and water of oceanic low-level clouds, *Science*, 363, eaav0566, <https://doi.org/10.1126/science.aav0566>, 2019.

Smalley, K. M., Lebsock, M. D., and Eastman, R.: Diurnal Patterns in the Observed Cloud Liquid Water Path Response to Droplet Number Perturbations, *Geophysical Research Letters*, 51, e2023GL107323, <https://doi.org/10.1029/2023GL107323>, 2024.

Marine Low Clouds : Radiation, Turbulence, and Forecasting:

Wood, R. and Hartmann, D. L.: Spatial Variability of Liquid Water Path in Marine Low Cloud: The Importance of Mesoscale Cellular Convection, *Journal of Climate*, 19, 1748–1764,

<https://doi.org/10.1175/JCLI3702.1>, 2006.

Yuan, T., Remer, L. A., and Yu, H.: Microphysical, macrophysical and radiative signatures of volcanic aerosols in trade wind cumulus observed by the A-Train, *Atmospheric Chemistry and Physics*, 11, 7119–7132, <https://doi.org/10.5194/acp-11-7119-2011>, 2011.

Zhang, J. and Feingold, G.: Distinct regional meteorological influences on low-cloud albedo susceptibility over global marine stratocumulus regions, *Atmospheric Chemistry and Physics*, 23, 1073–1090, <https://doi.org/10.5194/acp-23-1073-2023>, 2023.

Zhang, X., Wang, H., Che, H.-Z., Tan, S.-C., Yao, X.-P., Peng, Y., and Shi, G.-Y.: Radiative forcing of the aerosol-cloud interaction in seriously polluted East China and East China Sea, *Atmospheric Research*, 252, 105405, <https://doi.org/10.1016/j.atmosres.2020.105405>, 2021.

Zheng, Y., Rosenfeld, D., and Li, Z.: Estimating the Decoupling Degree of Subtropical Marine Stratocumulus Decks From Satellite, *Geophysical Research Letters*, 45, 12,560–12,568, <https://doi.org/10.1029/2018GL078382>, 2018.